Anticancer activity of alkynylgold(I) with P(NMe$_2$)$_3$ phosphane in mouse colon tumors and human colon carcinoma Caco-2 cell line.

Elisa Abas,[a] Natalia Espallargas,[a] Gianluca Burbello,[b] Jose E. Mesonero,[b,c,d] Antonio Rodriguez-Dieguez,[e] Laura Grasa,*[b,c,d] and Mariano Laguna.*[a]

[a] Instituto de Síntesis Química y Catálisis Homogénea, Universidad de Zaragoza-CSIC, Plaza S. Francisco s/n, 50009, Zaragoza, Spain.

[b] Dpto. Farmacología y Fisiología, Facultad de Veterinaria, Universidad de Zaragoza, Miguel Servet, 177, 50013, Zaragoza, Spain.

[c] Instituto de Investigación Sanitaria de Aragón (IIS Aragón), 50009, Zaragoza, Spain.

[d] Instituto Agroalimentario de Aragón -IA2- (Universidad de Zaragoza-CITA), 50013, Zaragoza, Spain.

[e] Dpto. de Química Inorgánica, Facultad de Química, Universidad de Granada, Severo Ochoa s/n, 18071, Granada, Spain.

ABSTRACT

New alkynylgold(I) with $P(NMe_2)_3$ (HMPT) phosphane complexes, [Au(C≡C-R)(HMPT)] (R= 4-Ph, 4-MePh, 4-OMe, 4-Br, 4-Cl, 2-py and 3-py) have been synthesized and characterized, including X-Ray studies of complexes with R= 4-OMe and 4-Br; besides their physicochemical properties and anticancer activity have been tested. Due to the great water solubility of the HMPT phosphane, all the complexes exhibit an optimal balance hydrophilicity/lipophilicity. Besides, all these complexes are quite stable in physiological conditions and interact strong enough with the transport protein BSA. All complexes exhibit a higher anticancer activity against Caco-2 cells than cisplatin, and some of them do not present cytotoxic activity against enterocyte-like differentiated cells. The selective complexes are proapoptotic drugs by the exposure of phosphatidylserine, results that are also confirmed in primary cultures from mouse colon tumors. Complexes with halogen unit also arrest the cell cycle in G2/M phase. It is thought that maybe this apoptosis processes are promoted by the observed oxidative damage in the membrane lipids, as a consequence of the inhibition of the thioredoxin reductase enzyme. Based on our results, we conclude that five of our complexes are good candidates to be used in chemotherapy.

INTRODUCTION

The most recent estimates of the worldwide burden of cancer (GLOBOCAN 2012) indicate that colorectal cancer (CRC) is the third most commonly diagnosed cancer, after lung and breast cancer, and the fourth highest cause of cancer death only after lung, liver, and stomach cancer.[1] According to these values it is still shocking that there is not a drug capable of fighting against cancer by itself, and in clinical practice, adjuvant chemotherapy with cytotoxic agents such as oxalilplatin in combination with fluorouracil (FU) and leucovorin (LV) or capecitabine, is a

standard of care for colon cancer patients in stage III.[2] Nevertheless, this treatment in stage II patients is still controversial.[3] Chemotherapy based on platinum drugs has been hampered by a decrease of sensitivity to these agents, which is attributed to diminished cellular drug accumulation, increased intracellular drug detoxification and increased DNA repair.[4] Besides, serious side effects are provoked as a result of the coordination of platinum center to N-atom of the DNA bases. To overcome these drawbacks, new researches have moved forward to other molecules and metals to avoid the development of this resistance by changing the target or action mechanism. Ruthenium with complexes such as NAMI-A, KP1019 or RAPTA-C presents an incredible anticancer activity; but other metals like osmium, copper, palladium or even gold are also being investigating due to their promising anticancer properties.[5-7] Gold compounds have a long and important tradition in medicine, although its medical application was reduced only for the treatment of severe rheumatoid arthritis.[8] However, the real need to achieve an effective anticancer drug, impulse gold researchers to develop new stable gold complexes. Gold is presented in different oxidative states, but only +1 and +3 are biologically relevant. Gold(I) is a soft cation with a preference for soft ligands, and this is why gold(I) chemistry is based on thiolate or phosphane ligands. Some examples of medicinally relevant gold(I) compounds are auranofin, aurothiomalate or aurothioglucose (**Figure 1**). Auranofin is known to inhibit the growth of different cancer cells *in vitro*, and also was reported to effectively increase the lifespan of mice inoculated with the lymphocytic leukemia P388 cells in a dose dependent manner.[9] Nevertheless, and although auronafin *in vivo* experiments were not so successful,[10] the design of this complex promoted the investigation of gold(I) with phosphane or thiolate ligand, due to their high selectivity and cytotoxicity.
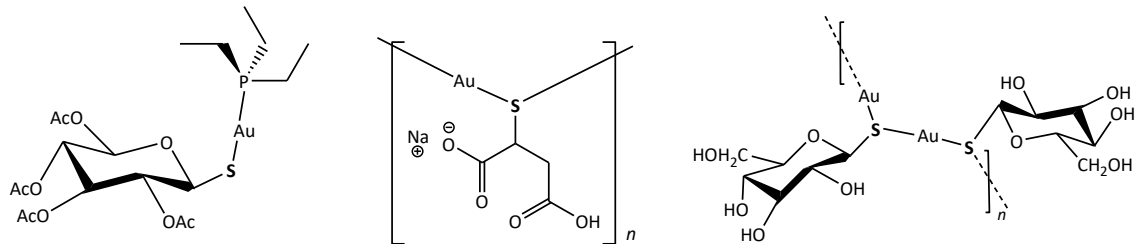
Figure 1. Structures of auranofin (left), aurothiomalate (middle) and aurothioglucose (right).

Ott's research group reported the role of the triethylphosphanegold(I) moiety with *N*-(*N',N'*-dimethylaminoethyl)-1,8-naphtalimide ligand, an anticancer agent by DNA intercalation.[11, 12] Besides, other research group also detailed the synthesis and the cytotoxic evaluation of Au(I) complexes bearing a diphenylphosphanoaminoheterocycle ligand associated to thiolate functionalized pyridine or nucleic bases.[13] In our group of investigation, several studies have been carried out with different phosphane ligand, especially PTA derivatives.[14-19] The auxiliary ligand present in the complex plays an important role because its nature will affect the compound lipophilicity and stability and the binding affinity of gold(I), and hence the intracellular transformation of gold(I) species and thus, the action mechanism.[8] Based on the need for the new drug to be water soluble, in order to be well-distributed in the organism, we selected the phosphane to work according to this property. Although other studies were performed with PTA ligand (1,3,5-triaza-7-phosphaadamantane),[17, 19, 20] in this study, we have focused on the hexamethylphosphorous triamide (HMPT), due to its higher water solubility (235 and 1000 g·l^{-1}, PTA and HMPT respectively). In addition to the Au-P bond, we decided to saturate the coordination sphere of the gold atom with different aromatic acetylene groups. Alkynyl gold(I) derivatives have been investigated due to their great antiproliferative effect of gold(I) alkynyl

phosphane complexes on several tumor cell lines.[21-24] In our investigation, the chosen alkynyl moiety is aromatic, in order to balance the lipophilicity and hidrophilicity properties, and also because of their potential luminescent properties. The alkynyl group may also present oxygen atom in its molecule to increase the water solubility of the final gold(I) complexes.[25-28]

Although gold(I) complexes mechanism is still under consideration, most of them seem to modify the oxidative conditions of the cells.[29] Based on the high affinity of the electrophilic gold center of gold(I) complexes to the nucleophilic sulfur and selenium containing residues, a covalent interaction to the selenocysteine residue of the thioredoxin reductase (TrxR) seems a possible action mechanism of these compounds. In fact, it is established that auranofin is a strong and selective TrxR inhibitor.[30, 31] TrxR system plays an important role as antioxidant system what is an additional advantage respect to other targets, because cancer cells are more active than healthy cells, and as a result of this, they produce more oxidant species. Thus, antioxidant systems are overexpressed to balance the increase of oxidative stress situation. In this way, the antioxidant enzyme thioredoxin reductase is overexpressed in cancerous cells.[32] This fact allows the drugs acting through this action mechanism of TrxR to show a higher selectivity for this population of cells and minimizes the severe side effects of the current chemotherapic agents.[33]

RESULTS AND DISCUSSION

Synthesis and Characterization. The entry point to the synthetic procedures is the synthesis of [AuCl(HMPT)] (**1**). Here, we proposed a new method for the complex **1** than the previously reported.[34] This reaction has to be done in argon atmosphere because free HMPT is quite sensitive to the air oxygen, and form the oxidized phosphane. Nevertheless, once the HMPT is coordinated to the gold center, this sensibility disappears. Tetrahydrothiophene (tht) ligand is effortless

substituted by HMPT phosphane in order to obtain the starting material **1**. Additionally, complex **1** can further be easily transformed to either alkynyl derivatives in ethanol solution, complexes that have not previously been reported, and their synthesis is summarized in **Scheme 1.**
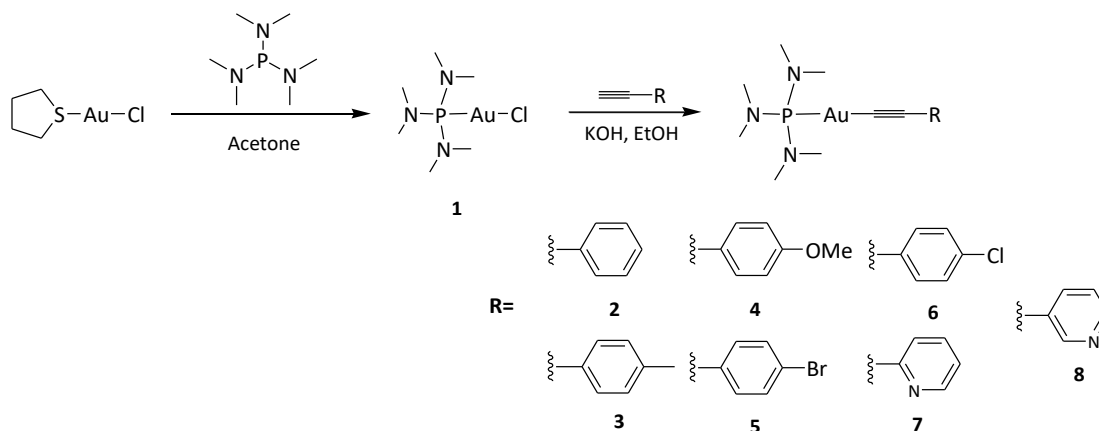
Scheme 1. Synthetic method for complexes 1 - 8.

All complexes are quite stable at room temperature and enough soluble in organic solvents. In both complexes the ligand is in its deprotonated form and coordinated to metallic center as it is shown by the IR and ^{1}HNMR spectra. The IR spectrum of complex **1**, in the low frequency region, is characterized by the presence of a strong band at 320 cm^{-1} due to Au−Cl stretching vibration (**Figure S1**). This band disappears after the reaction with the alkynyl ligand and a weak band at up to 2100 cm^{-1} corresponding to the C≡C bond appears, something that confirms the coordination. In addition, all complexes were characterized by ^{1}HNMR spectra and the corresponding signal of the tetrahydrothiophene ligand also disappears and the unequivocal doublet of the 18 protons of the HMPT ligand emerges. Besides, the resonances corresponding to the aromatic signals, the methyl (complex **3**) and methoxi group (complex **4**) are perfectly appreciable. Additional ^{31}P{H}NMR studies only showed the one signal of the phosphane, and a low shield shift of the doublet corresponding to the HMPT is observed as a result of the substitution of the chloride atom (**Table 1**).

Table 1. Shift of the HMTP signal in $^{31}P\{H\}$NMR.

$^{31}P\{H\}$NMR	1	2	3	4	5	6	7	8
δ(ppm)	110.87	133.46	133.23	135.24	133.24	133.18	133.12	132.92

APT-NMR spectra are also interesting because in most of the complexes with phenyl ring, we were able to distinguish the doublet corresponding of the coupling of C_β of the acetyls moiety and the phosphane. Quaternary carbons are always difficult to see, but C_α and C_β signals are especially problematic because of their poor electronic density, this effect is more pronounced in C_α due to its coordination to the metallic center, and that is why we are not capable to see them. The different groups present in the aromatic ring of these complexes also exhibit an influence on the C_β shifts as it can be seen in **Table 2**, halogen atoms (complex **5** and **6**) induce a higher shield shift of the C_β signals compared to the phenyl group (complex **2**). Besides, coupling constants between the phosphane and alkynyl group are coherent with other studies from the literature.[23, 35]

Table 2. Shift of the C_β signals in APT-NMR.

APT-NMR	2	4	5	6
δ C_β (ppm)	105.06	104.79	103.73	103.66
J_{C-P} (Hz)	32.3	32.3	33.3	28.3

For a fully characterization of the complexes, additional MALDI$^+$ mass spectrometry studies were performed. All complexes showed a signal attributed to the adduct [M+Au(HMTP)]$^+$ m/z (%)= 851.3(50.7) (2), 865.5 (42.2) (3), 881.3 (21.4) (4), 929.2 (17.8) (5), 855.2 (26.1) (6), 882.4 (59.9) (7) and 882.7 (17.7) (8).

Crystal Structure. We determined the crystal structures of gold complexes **4** and **5** by single-crystal X-ray diffraction. Both molecular structures are depicted in **Figure 2**. Compound **4** crystallizes (**Figure 2**, left) in the monoclinic group $P2_1/c$. The asymmetric unit consists of one unit of [Au(4-OMe-Phenylacetylene)HMPT]. The Au^I ions are two-coordinated and adopt a linear geometry in which the OMe-Phenylacetylene and the HMPT act as monodentate ligands and coordinate to the gold ions *via* the C7 and P1 atoms, respectively. The bond distances Au1-C7 and A1-P1 have values of 2.007(6) and 2.2732(13) Å, respectively, whereas C7-Au1-P1 bond angle is 173.55(16)°. Must be noted that C8-C7-Au1 bond angle has a value of 170.3(5)° generating a final angle of 70.71° between the plane containing the benzene ring and the defined plane for nitrogen atoms pertaining to the HMPT ligand (**Figure S2**).
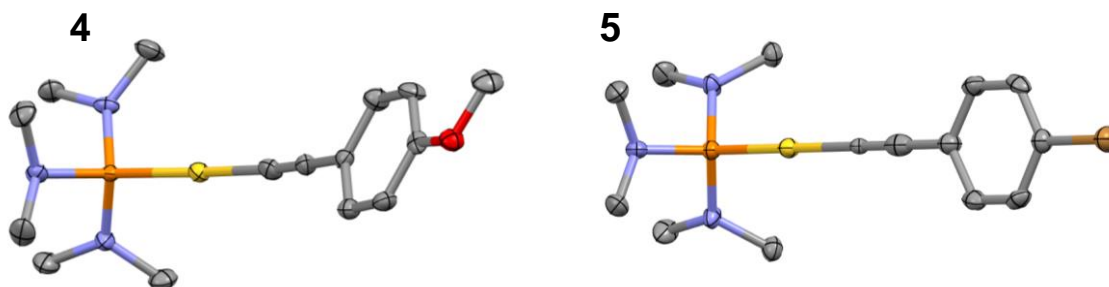

Figure 2. Molecular structures of complexes **4** (left) and **5** (right). The hydrogen atoms have been omitted for clarity. Thermal ellipsoids are drawn at the 50% probability level. Color code: N, blue; C, grey; O, red; Br, brown; Au, yellow.

Compound **5** crystallizes (**Figure 2**, right) in the monoclinic group $P2_1/m$. The asymmetric unit consists of half of Au atom, half 4-Br-Phenylacetylene and half HMPT ligand. The Au^I ions are two-coordinated and adopt a linear geometry in which the Br-Phenylacetylene and the HMPT act as monodentate ligands and coordinate to the gold ions *via* the C1 and P1 atoms, respectively. The bond distances Au1-C1 and A1-P1 have values of 2.052(7) and 2.272(2) Å, respectively, whereas

C1-Au1-P1 bond angle is 179.76(18)º. Must be noted that, in this case, C2-C1-Au1 bond angle has a value of 179.2(7)º generating an almost perpendicular angle of 86.45º between the plane containing the benzene ring and the defined plane for nitrogen atoms pertaining to the HMPT ligand (**Figure S2**).

As it can be observed in **Table 3**, Au(I) centres are coordinated to acetylene and phosphane group in a slightly distorted lineal geometry, especially for complex **4**. The distances between Au-P and Au-C are quite similar, which means that there is no difference in strength bonds.

Table 3. Selected bond lengths (Å) and angles (deg) of complexes **4** and **5.**

	[Au(4-OMe-Phenylacetylene)HMPT] (4)	[Au(4-Br-Phenylacetylene)HMPT] (5)
Bond lengths (Å)		
Au-P	2.2732(13)	2.272(2)
Au-C	2.007(6)	2.052(7)
C≡C	1.194(8)	1.137(12)
Bond angles (deg)		
C-Au-P	173.55(16)	179.76(18)
Au-C≡C	170.3(5)	179.2(7)
C≡C-C	176.1(6)	179.8(9)

Solution Stability Studies. As the compounds were not so water soluble as we expected, all biological assays were performed with compounds dissolved in DMSO (10 mM), and then they were diluted in the corresponding buffer to a final concentration of 6 mM. The stability of alkynyl complexes was evaluated by UV-vis spectroscopy in two different media. The first experiment was carried out in PBS solution (pH=7.4) and 37 ºC within a range of 190–800 nm over 24 h. Although small variations of intensity were registered, there is no evidence of gold decomposition (there is no band over 580 nm) or new signals that can indicate the evolution to other complex.

Moreover, taking into account the more complex media used for cytotoxic studies, we perform the stability of the gold(I) complexes in PBS with 20 % (*v/v*) complete medium (Supplemented Dulbecco's Modified Eagles medium (DMEM) see Experimental Section). This medium was selected because it is the culture medium of Caco-2 cells and it is important to test if the complexes are stable in this medium in order to determine possible changes in the structure according with prodrug behavior. The medium itself presents three bands at 212, 238 and 272 nm, so recorded spectra for all the gold(I) complexes are drastically different from the one obtain with only PBS due to these bands. In addition, the comportment observed of the complexes in this medium change in some cases. All the gold(I) derivatives with phenyl ring and also complex **8** (**Figure 3B**) experimented an intensity reduction of the bands related to the $\pi^*\leftarrow\pi$ transitions, and also hyperchromic effect of the band at 300 nm, especially for the complex **6** (**Figure 3A**). This modification is usually correlated to the formation of gold–oxygen bonds, as a result of hydrolysis process.[36] However, in the UV-vis spectrum of complex **7**, no significant modifications of the position and/or intensity of the bands were detected beyond 24 h, thus highlighting the compound stability in this solvent. Therefore, if the complex does not experiment changes in its structure, it may indicate that the active specie is the proposed structure for complex **7**, and no pro-drug behavior is operated. Some reactions of decomposition or reduction were observed in complex **2** and **5-6**, but not in the case of the complexes with pyridine ring.
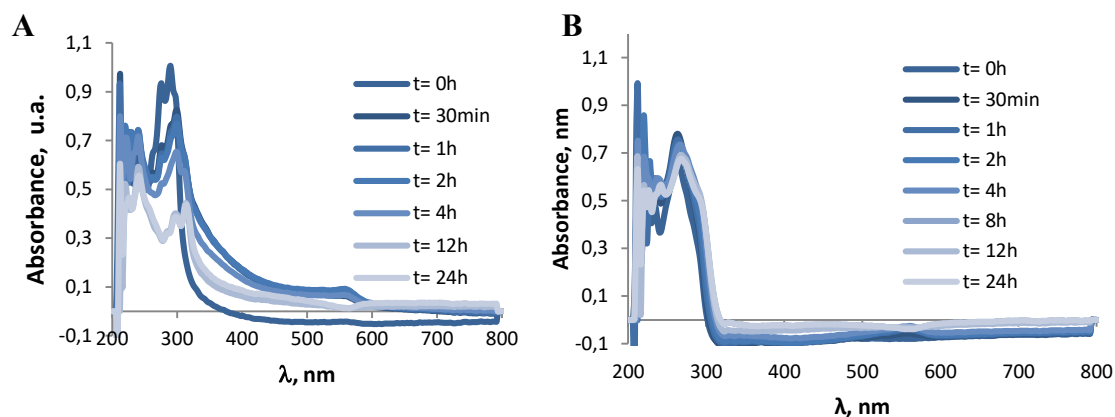
Figure 3. Stability studies of complex **6** (**A**) and complex **8** (**B**) in PBS with 20 % (*v/v*) complete medium. *More detailed in Supporting Information.*

Water solubility. In addition to stability studies, further studies about the physico-chemical properties of the complexes are needed to know if our molecule is a potential anticancer drug, such as water solubility and the lipophilicity/hydrophilicity relationship. Water solubility is indispensable for a well distribution in bloodstream, which allows reach the target. Cheng and Merz established the relationship between solubility and drug-likeness by the calculation of the $Log(S_W)$ parameter,[37] which should be from -6 (a little bit low) to 0 (optimal value). All the complexes synthesized in this work present very similar $Log(S_W)$ values, which are in the range of good drug-likeness (**Table 4**).

Table 4. $Log(S_W)$ values for gold(I) derivatives.

Complex	2	3	4	5	6	7	8
$Log(S_W)$	-3.49	-3.54	-3.39	-3.75	-3.69	-3.29	-3.22
$Log\ P_{o/w}$	0.63	1.33	0.66	0.91	1.03	1.24	1.20

Determination of Log P$_{o/w}$. As stated in the introduction, a balanced relationship between lipophilicity and hydrophilicity is crucial in drug delivery process. A high hydrophilicity may hamper a drug to penetrate biological membranes, thus affecting not only its activity but also its toxicity toward the healthy tissues. On the contrary, a high lipophilicity may hinder biomedical applications related to well-distribution profile. Furthermore, it is directly related to the plasma protein binding and metabolism of the drug.[38] This relationship was measured and investigated in terms of Log P$_{o/w}$ values, by using the shake-flask technique.[39, 40] This method studies the distribution of the complex between an equal amount of octanol and aqueous solution. Previous studies on phosphane gold(I) derivatives are great examples of the impact of high lipophilicity on the host toxicity,[41] resulting in drug accumulation in the mitochondria.[42] Consequently, a balanced relationship between the lipophilicity and hydrophilicity would be important in a drug-delivery process. Ideal values for Log P$_{o/w}$ parameter are between $-1 \leq \log P \leq 3$, although it is recommended for a greater oral and intestinal absorption values around 1.35-1.80.[43] All the tested compounds are lipophilic enough to satisfy the general lipophilicity requirement of drugs (**Table 4**). Complexes **3**, **7** and **8** are the more lipophilic ones, something that may indicate a higher permeability through the lipid bilayer than the rest of gold(I) derivatives.

Bovine Serum Albumin Interaction. In drug development, it is essential to study the ADME-tox profile of the complex deeply, in order to understand how the complex will behave in the organism.[44] One of these aspects is the distribution or transport mechanism of the compound to reach its target. In the circulatory system, the albumin is the most abundant protein (52-60 %),[45] and it is involved in control of osmotic blood pressure and the transport of various endogenous compounds as fatty acids, hormones, amino acids, etc. But serum albumin is also considered the most active protein in transport of exogenous drugs.[46, 47] Thus, analyses of the interaction of the

complexes with albumin are required. For these studies bovine serum albumin (BSA) is used instead of the human analogue (HBA). Both proteins contain a tryptophan in the subdomain IIA (Trp214 for HSA and Trp213 for BSA), but BSA presents an additional tryptophan residue (Trp 134) located on the surface which confers better fluorescent properties.[48] The Trp fluorescence is environmentally sensitive and changes in its atmosphere can result in signal quenching that can be used to study a possible interaction between BSA and our complexes. To perform these tests, we recorded the BSA fluorescence spectrum in the range of 310−450 nm upon excitation at 295 nm, and thereafter in the presence of increasing amounts of the gold complexes. No changes in the shape or position of the maximum were detected but a concentration-dependent quenching was observed for all tested complexes, as it can be seen for complex **2** in **Figure 4A**. This quenching was evaluated by the plot of Stern-Volmer equation to calculate K_{SV} and kq parameters (**Figure 4B** and **Table 5**). The kq is especially important because this value allows to determine the different operated quenching mechanism, static or dynamic. The establishment of a static or dynamic quenching could indicate the presence of the compound-BSA complex (static quenching) or only collisions between them (dynamic quenching).[49] The bimolecular quenching constant, kq, represents the efficiency of quenching or the accessibility of the fluorophore to the quencher, and due to the fact that dynamic quenching is diffusion controlled, higher values of kq than the diffusion-controlled rate constant of the biomolecule in water, 10^{10} M^{-1} s^{-1}, may imply that static quenching operates. According to our studies, the values of kq are on the order of 10^{12} M^{-1} s^{-1} (**Table 5**), confirming the interaction between both gold(I) complexes and BSA.
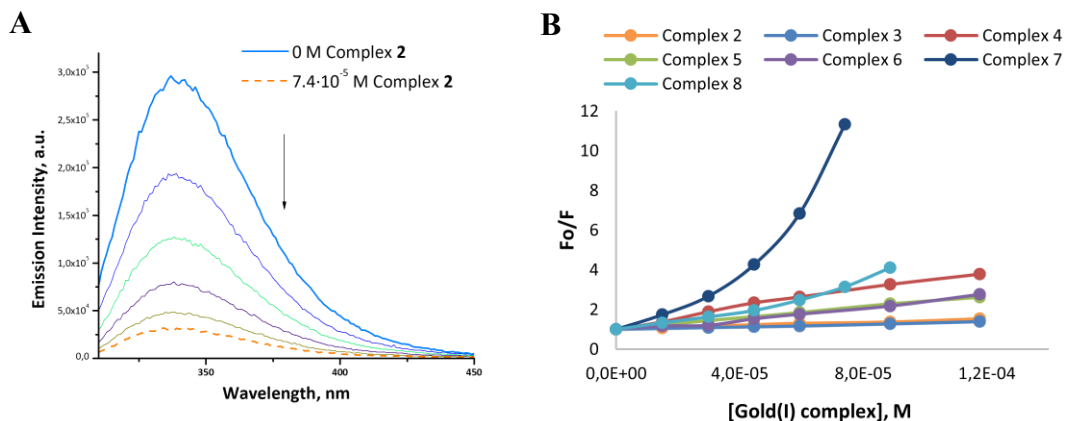
Figure 4. Fluorescence emission spectra of BSA at 298 K in the presence of different concentrations of complex **2** (**A**). Stern−Volmer plots for the quenching of BSA with increasing amounts of gold(I) complexes (complex concentration from 0 to 117 (**2-6**), 74 (**7**) and 88 (**8**) μM) at 298 K (λexc = 295 nm, [BSA] = 50 μM) (**B**).

Table 5. Values of the Stern−Volmer quenching constant (K_{SV}), bimolecular quenching constant (K_q), number of binding sites (n), binding constant (Kb), and thermodynamic parameters ($\Delta H°$, $\Delta S°$ and $\Delta G°$) for the interaction of gold(I) complexes with BSA.

Complex	K_{sv} (M^{-1})	k_q (M^{-1} s^{-1})	n	Kb (M^{-1})	$\Delta H°$ (KJ/mol)	$\Delta S°$ (KJ/mol)	$\Delta G°$ (KJ/mol)
2	$4.21 \cdot 10^4$	$4.21 \cdot 10^{11}$	0.95 (1)	$2.97 \cdot 10^3$	-205.90	-0.62	-19.81
3	$3.23 \cdot 10^3$	$3.23 \cdot 10^{10}$	0.77 (1)	$4.24 \cdot 10^2$	236.83	-0.71	-26.39
4	$2.38 \cdot 10^3$	$2.38 \cdot 10^{10}$	0.96 (1)	$1.73 \cdot 10^4$	48.07	-24.33	-24.17
5	$1.39 \cdot 10^4$	$1.39 \cdot 10^{11}$	0.97 (1)	$1.12 \cdot 10^4$	-78.02	-0.18	-23.10
6	$1.50 \cdot 10^4$	$1.50 \cdot 10^{11}$	1.22(1)	$1.01 \cdot 10^5$	-130.72	-0.34	-28.55
7	$7.19 \cdot 10^4$	$4.21 \cdot 10^{12}$	1.34 (1)	$3.68 \cdot 10^6$	100.16	0.45	-34.46
8	$3.32 \cdot 10^3$	$3.32 \cdot 10^{12}$	1.24 (1)	$2.68 \cdot 10^5$	44.84	0.25	-30.97

Once the interaction between the gold(I) derivatives and BSA was confirmed, additional studies were needed in order to determine not only the strength of these bindings but also the thermodynamic parameters. Evaluation of the strength of the interaction is indispensable because BSA must be only a transporter, but if the bond with the drug is too strong, BSA would be a kidnapper of the complex, avoiding the access to its target. Besides, as it was mentioned before, BSA contains different domains where drugs can bind, and thus more than one drug can be linked to the BSA. Modified Stern-Volmer equation plot (**Figure 5**) permits to calculate the values of the binding constant (Kb) for each experiment and the number of binding sites (n) (**Table 5**). The huge importance of the structure of the complex is clearly demonstrated in these results, showing that the slightly change from the bromide atom to chloride atom reduces the strength of the interaction with BSA 10-fold. However, the Kb values are in the range of 10^5-10^6, indicating an adequate strength of the binding BSA-complexes. By using the modified Stern−Volmer equation, it was also calculated the parameter *n*. According with our results, there is only one gold molecule coordinated to one molecule of BSA (1:1), and this bond is in agreement with those observed for other gold(I) derivatives,[14, 15] but slightly higher than the binding constant of *cis*platin.[50]
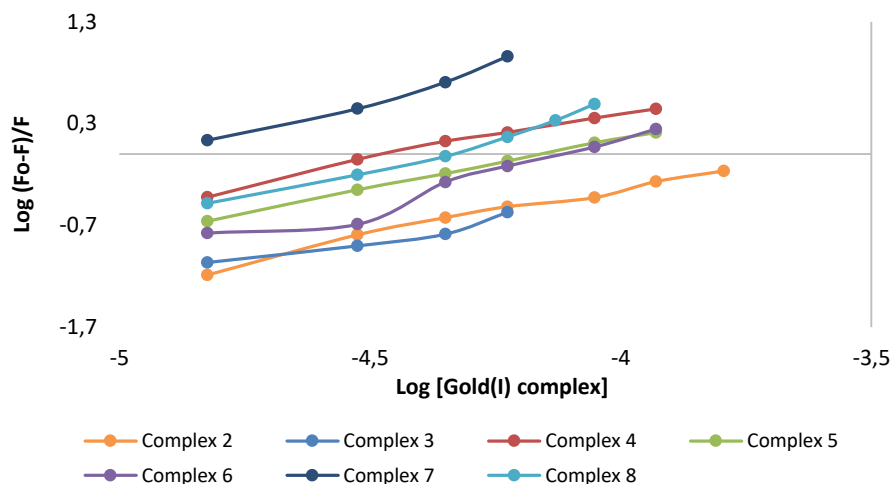
Figure 5. Modified Stern−Volmer equation plots for the quenching of BSA with increasing amounts of gold(I) complexes ((complex concentration from 0 to 117 (**2-6**), 74 (**7**) and 88 (**8**) μM)) at 298 K (λexc = 295 nm, [BSA] = 50 μM).

Additional thermodynamic studies were performed to know what kind of interaction is established between the gold complexes and BSA. The interaction forces between drugs and biomolecules may involve hydrophobic forces, electrostatic attraction, van der Waals interactions and hydrogen bonds. By characterizing the signs and magnitudes of the ΔH and ΔS parameters, it is possible to distinguish the operating interactions in protein association process.[51] If $\Delta H > 0$ and $\Delta S > 0$, hydrophobic interactions can be considered as the main forces; whereas if $\Delta H < 0$ and $\Delta S < 0$, van der Waals and hydrogen-bonding interactions are working in the reaction. Electrostatic forces are more dominant when $\Delta H < 0$ and $\Delta S > 0$. If the temperature barely changes, the enthalpy change (ΔH) can be considered as a constant, and then the free energy change (ΔG), the enthalpy change (ΔH) and the entropy change (ΔS) can be calculated according to Van't Hoff and Gibbs free energy equations, and all these values are collected in **Table 5**.

16

For all complexes tested, the binding with BSA seems to be a spontaneous process, as the free energy change (ΔG) is negative. Besides, the entropy change (ΔS) is also negative, indicating that the binding occurs in an exothermic process. Regarding the signs of ΔH and ΔS, we can assume that the forces involved are van der Waals interactions in the case of complexes **2**, **5** and **6**. Complexes **7** and **8** present positive entropy and enthalpy change, so hydrophobic interactions may be operating. This binding involves an endothermic reaction as it is shown by the positive enthalpy change (ΔH) found.

In Vitro Cytotoxic Activity. The cell line used to test the antiproliferative effect of complexes was the human colon adenocarcinoma cell line: Caco-2, clone TC7.[52, 53] This cell line is appropriate for our studies because it undergoes spontaneous enterocytic-like differentiation when it is cultured over confluence for 15 days to become polarized cells expressing apical and basolateral surfaces with well-established tight junctions, characteristics of normal epithelial cells.[53, 54] For this reason, Caco-2/TC7 allows us to study the antiproliferative effect not only on cancer cells (5 days after seeding) but also on considered normal epithelial cells (15 days after seeding). Cell proliferation was measured using the well-established MTT protocol.[55] The assay is dependent on the cellular reduction of 3-(4,5-dimethyl-2-thiazoyl)-2,5-diphenyltetrazolium bromide by the mitochondrial dehydrogenase of viable cells to a blue formazan product which can be measured spectrophotometrically. We investigated the cellular effects of the gold(I) complexes on undifferentiated (5 days) and differentiated (15 days) Caco-2/TC7 cells, after the exposure to the complexes for 72 h at different concentrations (0-20 μM in DMSO). According to **Table 6**, our results show that all gold(I) complexes are quite better than the actual chemotherapy based on cisplatin, as all of them present lower IC$_{50}$ (μM) values than cisplatin in this cell line (45.6$\pm$8.08),[7]

and what is more important, the majority are also selective for cancer cells (except for complex **3**), since no effect up to 20 µM on normal differentiated cells were detected. Based on these results, complex **3** was no longer considered a good candidate as an anticancer drug. Moreover, complex **7** reaches the strong cytotoxic effect registered for auranofin in cancer cells (2.10±0.40).[19] Besides, complex **4** was no tested due to problems of low yield.

**Table 6.** IC$_{50}$ values (µM) of gold(I) complexes.

Complex	2	3	5	6	7	8
IC50 cancer cells	3.72±0.08	4.02±0.18	5.25±0.21	6.14±0.14	2.33±0.10	6.26±0.15
IC50 normal cells	>>20	14.4±0.09	>>20	>>20	>>20	>>20

The results are expressed as mean values ± log SEM (n ≥ 12 experiments). NS: Not statistically significant.

Apoptosis studies in cancer cells. A balance between cell proliferation and death is needed to avoid different processes such as tumorigenesis. In a healthy organism, a hundred thousand cells are formed every second by mitosis, whereas the same amount of cells is destroyed by apoptotic process.[56] As it can be deduced, apoptosis is the appropriate cell death route and not necrosis because the first one avoids the release of the intracellular content to the extracellular medium, something that may imply inflammation, generally related to cancerous processes.[57] In this work we have studied two of the mechanisms involved in apoptosis: the externalization of phosphatidylserine (PS) through its interaction with annexin V-FITC and the activation of the caspase cascade. The lipid bilayer membrane presents an asymmetrical composition where PS is in the inner layer, but the exposure of PS to the outer leaflet of the plasma membrane is accepted as a universal characteristic of apoptotic cells.[58] This loss of asymmetry in the arrangement of phospholipids, with the consequent exposure of PS was observed for the first time in apoptotic

lymphocytes,[59, 60] and later confirmed for a large variety of cells such as cancer cell lines, vascular smooth muscle cells, etc.[57] Once exposed to the extracellular environment, binding sites on PS become available for annexin V, conjugated to a fluorochrome (FITC: fluorescein isothiocyanate), and using flow cytometry techniques, cells in stages of apoptosis can be identified. Besides, by the use of 7-Aminoactinomycin D (7-AAD) we can differentiate cell populations in early or late apoptosis. These experiments were carried out with undifferentiated cancer cells after the incubation with complexes **2**, **5-8** (20 μM) during 24 h and control cells were treated with the vehicle DMSO. As it can be seen in **Figure 6**, the complexes **5-8** but not complex **2**, exhibit a significant increase in population of cells undergoing apoptosis (in early and late stages) compared to control cells.
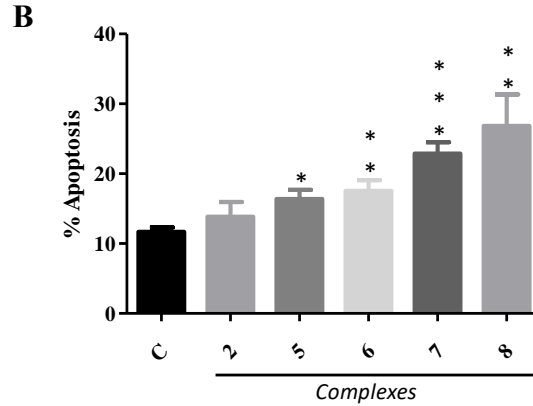
A

19

B
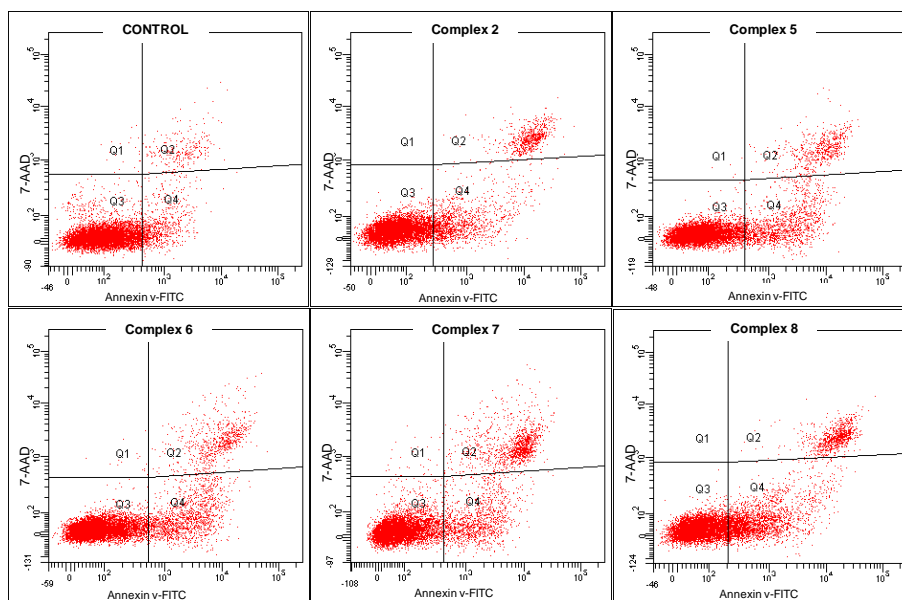
Figure 6. Fluorescence histograms of the distribution of cell populations in different stages: necrosis (Q1), living cells (Q3), late apoptosis (Q2) and early apoptosis (Q4), in control and gold(I) complexes treated Caco-2/TC7 cells (**A**). Apoptosis values, early + late, (%) of cells treated with gold(I) complexes (20 μM, 24 h). The results are expressed as mean values ± log SEM (n ≥ 4 experiments) *P<0.05; **P<0.01; ***P<0.001 vs. control. (**B**)

The above results indicate the proapoptic behaviour of our complexes by externalization of phosphatidylserine, but additional mechanisms of apoptosis can be held. Generally, there are two major pathways of apoptosis, the intrinsic and extrinsic pathways,[61, 62] but the two of them involve the activation of a cysteine proteases family named caspases. Caspases are a family of proteases (Cysteine-requiring Aspartate protease) that mediate cell death and are important for the process of apoptosis. Three different types of caspases can be distinguished: initiator caspases (caspases 2, 8, 9 and 10), executioner caspases (caspases 3, 6 and 7), and inflammatory caspases (caspases 1, 4, 5, 11 and 12). All of them were synthesized as an inactive form (pro-caspase), but inititator caspases can activate themselves, and start the caspase apoptotic pathway by triggering downstream caspases (executioner ones), which act as initial effectors during apoptosis to proteolytically dismantle most cellular structures.[63, 64] In the intrinsic and extrinsic pathways, although the initiator caspases of each pathway are different, both mechanisms mobilize the same

executioner caspases, caspases-3, -6 and -7. Thus, we focus our study on determining the activity of caspases-3 and -7 by luminescence assays.

Table 7. Caspase activity values (%) in control, staurosporine (STA, 1 μM, 4 h) and gold(I) complexes **2**, **5-8** treated Caco-2 cells (20 μM, 24 h).

	Control	STA	2	5	6	7	8
% activity	100±5.69	244.5±2.57***	8.22±3.64***	7.55±2.42***	10.16±2.05***	10.35±3.59***	8.22±2.44***

The results are expressed as mean values ± log SEM (n ≥ 4 experiments) ***$P<0.001$ vs. control.

The selected method is based on the production of free aminoluciferin by the action of caspase-3 and 7 on a DEVD-aminoluciferin substrate. The aminoluciferin is consumed by the luciferase, generating a luminescent signal that is proportional to caspase-3/7 activity. Staurosporine (STA, 1 μM, 4 h) was used as a positive control. Surprisingly, all the tested complexes induced a great decrease of the luminescence, compared to control cells (**Table 7**). These behaviours might be explained by a possible kidnap of the aminoluciferin, due to the different donor atoms present in the molecule,[65, 66] our complex may react with this specie and stop it from generating the corresponding signal, but additional studies should be performed to confirm this hypotheses.

Cell cycle studies. Since cell proliferation was inhibited by our complexes, we decided to investigate whether these compounds might induce any kind of alteration in the normal development of the cell cycle. Previous studies showed that some chemotherapeutics alter the different cycling-dependent kinases, responsible for the control of the cell cycle, which is usually related with an arrest in phase G2/M.[67] Our experiments carried out in cancer Caco-2/TC7 cells treated with gold(I) derivatives showed that while complex **2** does not have any effect on the cell

cycle, the complexes **5-8** alter it in different phases. In this sense, the complex **7** induces an arrest in S-phase, the complexes **5**, **6** and **8** induce an arrest in G2/M phase, since there is an increase in the number of cells in these phases, respectively, respect to control (**Figure 7** and **Table 8**). These results point out once more to the huge importance of the drug's structure, because by changing in one position the N atom, the mechanism of action changes drastically.
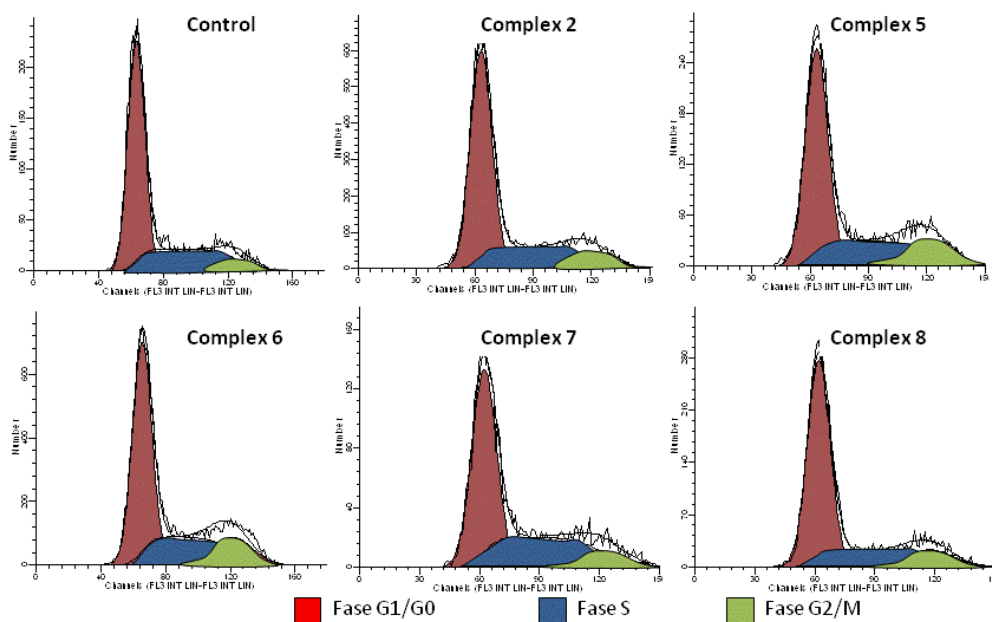

Figure 7. Fluorescence histograms obtained by flow cytometry of the cell populations in different phases of the cell cycle after 24 h of incubation of the cells with DMSO (control) and gold(I) complexes **2**, **5-8** (20 µM).

Table 8. Cell populations (%) in the different phases of the cell cycle.

Complex	G0/G1	S	G2/M
Control	60.25±1.53	33.02±1.25	6.73±0.55
Complex *2*	60.89±4.23	30.63±3.50	8.48±1.22
Complex *5*	53.82±2.11*	36.42±3.32	9.76±1.38*
Complex *6*	51.47±2.17**	38.50±3.32	10.03±1.38*
Complex *7*	51.58±1.87**	39.18±1.69**	9.23±1.61
Complex *8*	58.54±3.52	31.19±3.63	10.27±0.17***

The cells were treated with vehicle DMSO (control) or complexes 2, 5-8 (20 µM, 24 h). Values are expressed as mean values ± log SEM (n ≥ 4 experiments). *P<0.05; **P<0.01; ***P<0.001 vs. control.

Effects on Reactive Oxygen Species (ROS) generation. During the cellular process of division and respiration, ROS species are generated. These species have an enormous oxidizing effect but, in a well-functioning organism, the antioxidant system balances this effect and the ROS species imply a positive effect as a proapoptotic system for those cells that must be replaced.[68] Nevertheless, in high concentration, ROS can produce severe damage and even cell death by oxidizing their proteins, lipids or nucleic acids.[69-71] The increase of the ROS levels in the cell is provoked by a disruption on the antioxidant system, and it is usually known as oxidative stress. In order to determine the oxidative stress, we studied the generation of oxidized proteins and lipids.

Protein oxidation evaluation. The most established method to measure the oxidation of proteins is the quantification of carbonyl species.[72] In this investigation, we used 2,4-dinitrophenylhydrazine (DNPH) to generate 2,4-dinitrophenylhydrazone by the reaction with carbonyl groups present in the oxidized proteins. The resulting hydrazone can be detected by UV-

vis spectroscopy at 375 nm, which allows us to calculate the total content of carbonyl species of the protein present in the lysate. Although proteins are very sensitive biomolecules, no evidence of oxidative damage was observed with any of the gold(I) complexes used (**Figure 8A**). *Lipid peroxidation evaluation*. Lipids present in the membrane layer can also be easily oxidized to form peroxidised species such as malondialdehyde (MDA) and hydroxyalkenals (4-HDA), which are important biomarkers to evaluate oxidative damage in lipids. To quantify both biomarkers at the same time, we use Gerard-Monier method,[73] which is based on the condensation reaction between MDA or 4-HDA with two molecules of N-methyl-2-phenylindole. The resulting product can be measured by UV-vis spectroscopy at 586 nm. In contrast with the observed in carbonyl assay, now oxidative damage in lipids was observed for all the tested gold complexes (**Figure 8B**).
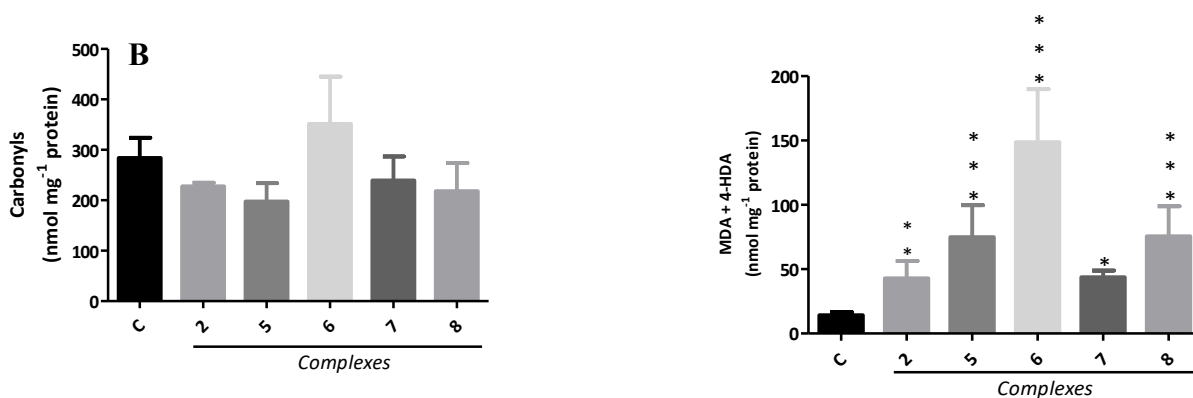

Figure 8. Carbonyl (**A**) and MDA+4-HDA (**B**) levels (nmol mg^{-1} protein) in Caco-2/TC7 cells treated with the vehicle DMSO (control) or the gold(I) complexes **2**, **5-8** (24 h, 20 μM). Values are expressed as mean values ± log SEM (n≥6 experiments). *P<0.05; **P<0.01; ***P<0.001 vs. control

Inhibition of TrxR system. As it was mentioned before, stress oxidative is the consequence of a disruption in the antioxidant/oxidant balance. The endogenous antioxidant system consists of

enzymatic antioxidants such as superoxide dismutase (SOD), catalase (CAT), glutathione peroxidase (GPx) or the family of thioredoxins (Trx). The latter, together with the glutarredoxin protein family, plays an important role in the maintenance of redox homeostasis through the exchange of dithiol disulfide with its target proteins.[74] Besides due to the presence of these thiol and selenothiol moieties, this protein might represent a good candidate to study, since gold tends to coordinate to these groups. Moreover, several studies point out that, due to the increased cellular proliferation and the high metabolic demand of the tumor cells, Trx system is overexpressed being a great new target for chemotherapy.[75] In contrast to other investigations, in which the capacity of the compounds to modify the activity of the Trx was tested on Trx isolated from rat liver,[76, 77] we determined the activity of Trx in cancer cells (Caco-2/TC7) treated with the complexes. This difference allows us to understand the complexes behavior in our *in vitro* model, the same used for the evaluation of stress oxidative damage. A strong decrease of the thioredoxin reductase (TrxR) activity was induced by all the gold(I) complexes compared with the basal activity registered for the control cells (**Figure 9**), which is consistent with the oxidative damage observed in membrane lipids.
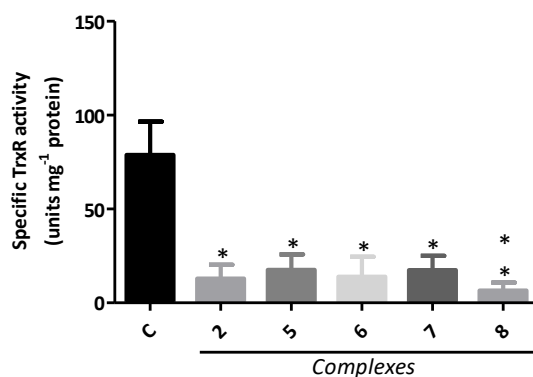

Figure 9. Specific TrxR activity (units mg-1 protein) in Caco-2/TC7 cells treated with gold(I) complexes (20 µM, 24 h). Values are expressed as mean values ± log SEM (n≥4 experiments). *P<0.05; **P<0.01 vs. control.

Apoptosis studies in primary cultures of mouse colon tumors. Based on the excellent results obtained with the complexes in Caco-2 cells, we decided to reevaluate the induction of the apoptosis by the mechanism of phosphatidylserine externalization in a mouse model, which is closer to the conditions of development of cancer in humans. One of the most widely used protocols for inducing colon cancer in mice is based on the administration of the carcinogenic azoxymethane (AOM) and dextran sulfate sodium (DSS) to induce epithelial damage. The combination of these two compounds generally produces a colonic tumorigenesis in a period of 10 weeks.[78, 79] In our experiments, a total of 5 mice survived and developed tumors, finding 3.25 ± 0.47 tumors/mouse with an mean size of 2.49 ± 0.34 mm of diameter. In some cases, some processes of metastasis in the peritoneal organs could be observed.

The isolated tumor tissue was subjected to enzymatic digestion to achieve viable individual cancer cells to be seeded in a culture plate. Then, the same protocol as in the *in vitro* model of cells was carried out to detect the exposure to phosphatidylserine. We found that all tested complexes induce apoptosis by phosphatidylserine signaling mechanism in primary cultures from mouse colon tumors, confirming the *in vitro* results obtained from Caco-2/TC7 cells (**Figure 10**).
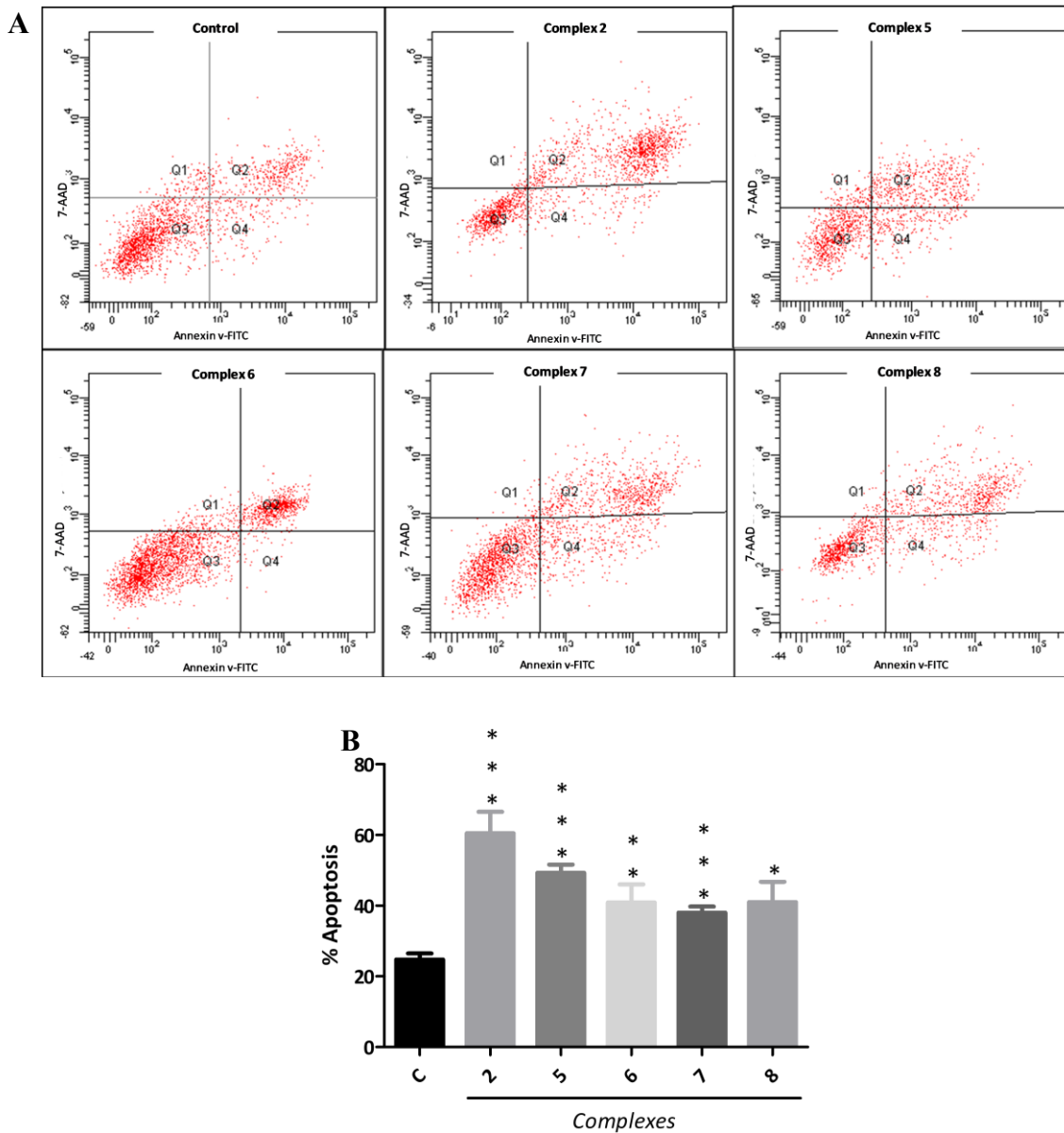
Figure 10. Fluorescence histograms of the distribution of cell populations in different stages: necrosis (Q1), living cells (Q3), late apoptosis (Q2) and early apoptosis (Q4), in control and gold(I) complexes treated Caco-2 cells (**A**). Apoptosis values, early + late, (%) of Caco-2 cells treated with gold(I) complexes (20 μM, 24 h). The results are expressed as mean values ± log SEM (n ≥ 4 experiments) *P<0.05; **P<0.01; ***P<0.001 vs. control. (**B**)

CONCLUSIONS

In this work, we describe the synthesis of seven novel gold(I)complexes with the water soluble phosphane HMPT and an ethynylphenyl or ethynylpyridine moiety. After their characterization, we have evaluated some of their ADME-tox profile properties: thermal stability, water solubility, lipophilicity, interaction with BSA, and their antiproliferative activity. Besides, their mechanism of action was studied in detail. All complexes showed much more cytotoxic activity than cisplatin in Caco-2/TC7 cells, and what is more, an exception of complex **3** they are no toxic drugs for considered normal epithelial cells (differentiated Caco-2/TC7 cells). The selective complexes induce apoptosis in undifferentiated cancer Caco-2/TC7 cells through the phosphatidylserine signaling pathway, and some of them induce alterations of the cell cycle. Complexes **2**, **5**, **6** and **8** arrest the cycle in G2/M phase whereas complex **2** arrests the cycle in S-phase. One more time, the huge importance of the drug's structure is clearly visible in these experiments, since the N atom position determines not only the antiproliferative effect of the drug but also its mechanism. Oxidative stress studies reveal that these complexes induce oxidative damage in membrane lipids, something that may be related with the strong inhibition of the antioxidant system TrxR also found. Finally, we detected a phosphatidylserine externalization in the cells from primary cultures of mouse colon tumors, confirming the *in vitro* studies. All of our results suggest that complexes **2** and **5-8** might be promising candidates for colon cancer chemotherapy.

EXPERIMENTAL SECTION

General procedures

NMR Spectroscopy. ^{1}H, ^{31}P and ^{13}C NMR spectra were recorded on 400 or 300 MHz Bruker Avance spectrometers and are referenced to external TMS or 85% H_3PO_4 (^{31}P), Chemical shifts (δ) are given in ppm, coupling constants are reported in Hz. MALDI mass spectra were measured

on a Micromass Autospec spectrometer in positive ion mode using DCTB (1,1-diciano-4-^{t}butylphenyl-3-methylbutadiene) as matrix. Infrared spectra (4000-250 cm^{-1}) were recorded on a Perkin Elmer Spectrum 100 FTIR (far-IR) spectrometer. Elemental analyses were obtained in-house using a LECO CHNS-932 microanalyser. The starting material: the phosphane HMPT was purchased from Alfa Aesar (Kandel, Germany) and the thiols were purchased from Sigma-Aldrich (Madrid, Spain) and used as received. [AuCl(tht)] were prepared according to published methods,[80] and [AuCl(HMPT)] with a slightly modified procedure.[34]

WARNING: Special care must be taken with the phosphane, thus working in a well-ventilated place is extremely recommended.

Synthesis and Characterization.

[AuCl(HMPT)] (**1**). To a suspension of [AuCl(tht)] (2 mmol, 0.643 g) in 20 mL of acetone in a shlenk tube under argon was added 3 mmol of HMPT (2 mmol, 0.489 g, 0.365 mL) and stirred for 1 h at room temperature. The resulting solution was evaporated until dryness and a white solid is observed. Yield: 93% white solid. ^{1}H NMR (400 MHz, CDCl$_3$) δ (ppm) 2.66 (d, J = 11.7 Hz, 18H). ^{31}P {^{1}H} NMR (162 MHz, CDCl$_3$) δ(ppm) 110.87 (s). APT-RMN (101 MHz, CDCl$_3$) δ(ppm) 37.79 (d, J=9.2 Hz) IR (ν(cm^{-1})): 2922, 1462, 1425, 1408, 1281, 1179, 1149, 1063, 958, 719, 677, 523, 316. MS (MALDI$^+$, m/z (%)):270.2 (58.8, [Au-PNMe$_2$]$^+$), 360.1 (46.2, [M-Cl]$^+$), 523.2 (100, [M-Cl+HMPT]$^+$), 755.1 (22.1, [2M-Cl]$^+$). S$_{25°C}$ H$_2$O (mg/L)= 496.6

Synthesis of alkynyl complexes (**2**)-(**8**). To a solution in ethanol, 20 mL, of the corresponding 4-R-Phenylacetylene (R= H (**2**), Me (**3**), OMe (**4**), Br (**5**) and Cl (**6**)) (0.2 mmol) or the ethynylpyridine group (2-ethynyl (**7**) and 3-ethynylpyridine (**8**)) was added an ethanol solution of

KOH (0.27 mmol, 0.155 g). After 30 min of stirring, [AuCl(HMPT)] (0.21 mmol, 0.84 g) was added and it is stirred for additional 24 h at room temperature, the corresponding solid was discarded by filtration and the crude was evaporated until dryness, and finally wash with distilled water and diethyl ether.

Complex **2**: Yield 70% ^{1}H NMR (400 MHz, CDCl$_3$) δ(ppm) 7.38 (d, J = 8.1 Hz, 2H), 7.03 (d, J = 7.9 Hz, 2H), 2.67(d, 18H), 1.62 (s, 3H).^{31}P {^{1}H} NMR (162 MHz, CDCl$_3$) δ(ppm) 133.23 (s).APT-RMN (101 MHz, CDCl$_3$) δ(ppm) 37.79, 104.84, 122.03, 132.29, 128.83, 136.68, 58.71 IR (ν (cm^{-1})): 2970, 2880, 2113, 1653, 1504, 1464, 1449, 1281, 1183, 1090, 1049, 968, 953, 816, 716, 677. MS (MALDI$^+$, m/z (%)): 523.3 (100, [Au(HMPT)$_2$]$^+$), 821.3 (50.67, [M+Au(HMPT)]$^+$). Anal.Calcd for C$_{14}$H$_{23}$AuN$_3$P (461.29): C, 36.45; H, 5.03; N, 9.11. Found: C, 36.57; H, 5.12; N, 9.23. S$_{25°C}$ H$_2$O (mg/L)= 150.6

Complex **3**: Yield 81% ^{1}H NMR (400 MHz, CDCl$_3$) δ(ppm) 7.38 (d, *J* = 8.1 Hz, 2H), 7.03 (d, *J* = 7.9 Hz, 2H), 2.67(d, 18H), 1.62 (s, 3H).^{31}P {^{1}H} NMR (162 MHz, CDCl$_3$) δ(ppm) 133.23 (s).APT-RMN (101 MHz, CDCl3) δ(ppm) 37.79, 104.84, 122.03, 132.29, 128.83, 136.68, 58.71 IR (ν(cm^{-1})): 2970, 2880, 2113, 1653, 1504, 1464, 1449, 1281, 1183, 1090, 1049, 968, 953, 816, 716, 677. MS (MALDI$^+$, m/z (%)): 523.4 (90.2, [Au(HMPT)$_2$]$^+$), 835.5 (42.2, [M+ Au(HMPT)]$^+$). Anal.Calcd for C$_{15}$H$_{25}$AuN$_3$P (475.32): C, 37.90; H, 5.30; N, 8.84. Found: C, 37.60; H, 5.25; N, 8.72. S$_{25°C}$ H$_2$O (mg/L)= 135.8

Complex **4**: Yield 31% ^{1}H NMR (400 MHz, CDCl$_3$) δ(ppm) 7.43 (d, *J* = 8.5 Hz, 2H), 6.77 (d, *J* = 5.5 Hz, 2H), 3.79 (s, *J* = 11.3 Hz, 3H), 2.66 (dd, *J* = 11.5, 5.1 Hz, 18H).^{31}P {^{1}H} NMR (162 MHz, CDCl$_3$) δ(ppm) 135.24 (s).APT-RMN (101 MHz, CDCl$_3$) δ(ppm) 37.81,104.63, 117.39, 133.75, 113.95, 158.53, 55.37 IR (ν(cm^{-1})): 2920, 2794, 2018, 1600, 1504, 1457, 1284, 1241, 1186, 1030, 975, 833, 706, 675. MS (MALDI$^+$, m/z (%)): 523.3 (95.2, [Au(HMPT)$_2$]$^+$), 655.3 (4.1,

[M+HMPT]$^+$), 851.3 (21.42, [M+Au(HMPT)]$^+$), 1342.7 (6.31, [2M+Au(HMPT)]$^+$). Anal.Calcd for $C_{15}H_{25}AuN_3OP$ (491.32): C, 36.67; H, 5.13; N, 8.55. Found: C, 36.59; H, 5.29; N, 8.62. $S_{25°C}$ H_2O (mg/L)= 198.2

Complex **5**: Yield 85% ^{1}H NMR (400 MHz, CDCl$_3$) δ(ppm) 7.35 (m, 4H), 2.68 (d, J = 11.3 Hz, 18H). ^{31}P {^{1}H} NMR (162 MHz, CDCl$_3$) δ(ppm) 133.24 (s).APT-RMN (101 MHz, CDCl$_3$) δ(ppm) 37.64, 103.41, 124.01, 133.57, 131.37, 120.54 IR (ν(cm^{-1})): 2994, 2787, 2116, 1671, 1473, 1455, 1445, 1276, 1241, 1174, 1060, 960, 835, 714, 676, 279. MS (MALDI$^+$, m/z (%)):523.4 (100, [Au(HMPT)$_2$]$^+$), 929.2 (17.8, [M+Au(HMPT)]$^+$). Anal.Calcd for $C_{14}H_{22}AuBrN_3P$ (475.32): C, 31.13; H, 4.10; N, 7.78. Found: C, 31.26; H, 4.27; N, 7.81. $S_{25°C}$ H_2O (mg/L)= 45.6

Complex **6**: Yield 98% ^{1}H NMR (400 MHz, CDCl$_3$) δ(ppm) 7.43 – 7.38 (m, 2H), 7.22 – 7.17 (m, 2H), 2.68 (d, J = 11.3 Hz, 18H).^{31}P {^{1}H} NMR (162 MHz, CDCl$_3$) δ(ppm) 133.18 (s).APT-RMN (101 MHz, CDCl$_3$) δ(ppm) 37.79, 103.66, 132.52, 133.09, 128.60, 123.7 IR (ν(cm^{-1})): 2993, 2787, 2116, 1674, 1475, 1455, 1445, 1278, 1174, 1061, 962, 951, 839, 715, 677. MS (MALDI$^+$, m/z (%)): 523.3 (100, [Au(HMPT)$_2$]$^+$), 855.2 (26.1, [M+ Au(HMPT)]$^+$). Anal.Calcd for $C_{14}H_{22}AuClN_3P$ (495.74): C, 33.92; H, 4.47; N, 8.48. Found: C, 33.74; H, 4.31; N, 8.54. $S_{25°C}$ H_2O (mg/L)= 101.7

Complex **7**: Yield 88% ^{1}H NMR (400 MHz, CDCl$_3$) δ(ppm) 8.49 (ddd, J = 4.9, 1.7, 0.9 Hz, 1H), 7.57 – 7.48 (m, 1H), 7.39 (dt, J = 7.9, 1.0 Hz, 1H), 7.07 (ddd, J = 7.5, 4.9, 1.2 Hz, 1H), 2.67 (d, J = 11.3 Hz, 18H). ^{31}P{^{1}H} NMR (162 MHz, CDCl$_3$) δ(ppm) 133.12 (s). APT-RMN (101 MHz, CDCl$_3$) δ(ppm) 37.8, 126.98, 135.66, 121.33, 149.72 IR (ν(cm^{-1})): 2994, 2883, 2789, 2118, 1581, 1558, 1572, 1458, 1420, 1281, 1238, 1182, 1147, 1064, 961, 951, 781, 717, 675. MS (MALDI$^+$, m/z (%)): 501.1 (99.2, [M+K]$^+$) 523.3 (95.6, [Au(HMPT)$_2$]$^+$) 822.7 (59.9, [M+Au(HMPT)]$^+$).

Anal.Calcd for $C_{13}H_{22}AuN_4P$ (462.28): C, 33.78; H, 4.80; N, 12.12. Found: C, 33.82; H, 4.72; N, 12.24. $S_{25°C}$ H_2O (mg/L)= 236.4

Complex **8**: Yield 80% ^{1}H NMR (400 MHz, CDCl$_3$) δ(ppm) 8.72 (s, 1H), 8.39 (dd, *J*=4.9 Hz, 1H), 7.74 (dt, *J* = 7.9 Hz, 1H), 7.16 (ddd, *J* = 7.9, 4.9, 0.8 Hz, 1H), 2.69 (d, *J* = 11.3 Hz, 18H). ^{31}P{^{1}H} NMR (162 MHz, CDCl$_3$) δ(ppm) 132.92 (s). APT-RMN (101 MHz, CDCl$_3$) δ(ppm) 37.75, 139.11, 122.79, 147.07, 153.32 IR (ν(cm^{-1})): 2882, 2788, 2118, 1653, 1578, 1559, 1471, 1400, 1281, 1226, 1183, 1150, 1062, 959, 808, 709, 675.MS (MALDI$^+$, m/z (%)):523.3 (48.11, [Au(HMPT)$_2$]$^+$) 822.4 (17.74, [M+Au(HMPT)]$^+$). Anal.Calcd for $C_{13}H_{22}AuN_4P$ (462.28): C, 33.78; H, 4.80; N, 12.12. Found: C, 33.85; H, 4.76; N, 12.27. $S_{25°C}$ H_2O (mg/L)= 280.7

Single-Crystal Structure Determination. Suitable crystals of 4 and 5 were mounted on a glass fibre and used for data collection on a Bruker AXS APEX CCD area detector equipped with graphite monochromated Mo Kα radiation (λ = 0.71073 Å) by applying the ω-scan method. Lorentz-polarization and empirical absorption corrections were applied. The data reduction were performed with the APEX2 software (Bruker Apex2, Bruker AXS Inc., Madison, Wisconsin, USA, 2004) and corrected for absorption using SADABS (G.M. Sheldrick, SADABS, Program for Empirical Adsorption Correction, Institute for Inorganic Chemistry, University of Gottingen, Germany, 1996). Crystal structure was solved by direct methods and refined by full-matrix least-squares on F2 including all reflections using anisotropic displacement parameters by means of the WINGX crystallographic package (G. M. Sheldrick, SHELX-2014, Program for Crystal Structure Refinement, University of Göttingen, Göttingen, Germany, 2014).[81] Generally, anisotropic temperature factors were assigned to all atoms except for hydrogen atoms, which are riding their parent atoms with an isotropic temperature factor arbitrarily chosen as 1.2 times that of the

respective parent. Final R(F), wR(F2) and goodness of fit agreement factors, details on the data collection and analysis can be found in Table S1. Selected bond lengths and angles are given in Table S2 (ESI). CCDC reference numbers for the structures of **4** and **5** were 1960425-1960424. Copies of the data can be obtained free of charge upon application to CCDC, 12 Union Road, Cambridge CB2 1EZ, U.K. (fax, (+44)1223 336-033; e-mail, deposit@ ccdc.cam.ac.uk).

Cell culture. This study was carried out in the human enterocyte-like cell line Caco-2/TC7,[82] kindly provided by Dr. Edith Brot-Laroche (INSERM, UMR S 872, Centre de Recherches de Cordeliers, Paris, France). This cell line undergoes in culture a process of spontaneous differentiation that leads to the formation of a monolayer of cells, expressing morphological and functional characteristics of the mature enterocytes. This differentiation process is growth-dependent, where the cells undergo differentiation from 'undifferentiated proliferative crypt-type cells' in exponential phase of growth, to 'differentiated enterocyte-type cells' in stationary phase.[83] Caco-2/TC7 cells (passages 30-50) were cultured at 37ºC in an atmosphere of 5% CO_2 and maintained in high glucose DMEM supplemented with 2 mM glutamine, 100 U/mL penicillin, 100 µg/mL streptomycin, 1% non-essential amino acids, and 20% heat-inactivated fetal bovine serum (FBS) (Life Technologies, Carlsbad, CA, USA). To cell line maintenance, cells were passaged enzymatically with 0.25% trypsin-1 mM EDTA and sub-cultured on 25 cm^2 plastic flasks at a density of 10^4 cells/cm^2. Culture medium was replaced every 2 days. With this density of culture, the cells reach cell confluence 90 % (where cell differentiation starts) at 7 days after seeding, and the complete cell differentiation is reached at 15 days post-seeding. Thus, experiments in undifferentiated and differentiated cells (considered as cancer and normal cells, respectively) were performed between 2-5 days and 12-15 days post-seeding, respectively. For cell viability assays,

cells were seeded in 96-well plates at a density of 2×10^4 or 4×10^3 cells per well, and measurements were carried out 5 or 15 days after seeding, respectively. For thioredoxin reductase and oxidative stress assays, cells were seeded at a density of 3.3×10^4 cells/cm^2; for apoptosis and cell cycle analyses at 3×10^4 cells/cm^2; and for caspase assays at 10^3 cells per well in 96-well plates. Stock solutions of the complexes (in DMSO) were diluted in the complete medium to the required concentration. DMSO at similar concentrations did not show any cytotoxic effects. The culture medium was replaced with fresh medium (without FBS) containing the complexes at concentrations varying from 0 to 20 μM, and with an exposure time of 72 h for cell viability assays. For all the other studies, the cells were incubated at 20 μM for 24 h.

Cell viability assay. Cell survival was measured by using the MTT test.[55] The assay is dependent on the cellular reduction of 3-(4,5-dimethylthiazol-2-yl)-2,5-diphenyltetrazolium bromide (MTT, Sigma-Aldrich, Madrid, Spain) by the mitochondrial dehydrogenase of viable cells to a blue formazan product that can be measured spectrophotometrically. Following the appropriate incubation of cells, with or without the metallic complexes, MTT (5 mg mL^{-1}) was added to each well in an amount equal to 10 % of the culture volume. Cells were incubated with MTT at 37 °C for 3 h. After that, the medium and MTT were removed and 100 μl of DMSO was added to each well. The plate was gentle stirred in a shaker. Finally, the cell viability was determined by measuring the absorbance with a multi-well spectrophotometer (DTX 800 Multimode Detector, Beckman Coulter) at a wavelength of 560 nm and compared with the values of control cells incubated in the absence of the complexes. IC$_{50}$ values were calculated using a conventional concentration-response curve with variable slope. Experiments were conducted in quadruplicate wells and repeated at least three times.

Apoptosis studies. For the studies of apoptosis, by means of the detection of phosphatidylserine in the outer layer of the plasma membrane, the Annexin V-FITC Apoptosis Detection kit (Immunostep, Spain) was used. After the incubation with the complexes, the cells were collected and transferred to flow-cytometry tubes. A negative control was prepared with untreated cells, that was used to define the basal level of apoptotic and necrotic or dead cells. The staining with Annexin V-FITC and 7-Aminoactinomycin D (7-ADD) was performed according to manufacturer's recommendation. The cells were washed twice with temperate phosphate-buffered saline (PBS) and resuspended in 200 µl of 1 x Annexin-binding buffer. Thereafter, 2.5 µl of the Annexin V-FITC and 2.5 µl of PI were added to each 50 µl of cell suspension. After incubation for 15 min at RT in the dark, 400 µl of 1 x Annexin binding buffer were added and analyzed by flow cytometry within 1 h. The signal intensity was measured using a Gallios Flow Cytometry (Beckman Coulter) and analyzed using the Kaluza Analysis Software (Beckman Coulter).

Cell cycle analyses. After the incubation with the complexes, the cells were collected, washed twice with PBS, fixed in 70% ice-cold ethanol and stored at 4 °C for 24 h. After centrifugation, cells were resuspended in PBS containing propidium iodide (PI, 50 µg/mL) and RNase A (100 µg/mL). After incubation for 30 min at RT in the dark, PI stained cells were analyzed for DNA content in a Gallios Flow Cytometry (Beckman Coulter). The red fluorescence emitted by PI was collected by 620 nm longer pass filter, as a measure of the amount of DNA-bound PI and displayed on a linear scale. Cell cycle distribution was determined on a linear scale. The percentage of cells in cycle phases was determined using the Kaluza Analysis Software (Beckman Coulter).

Caspase 3/7 activity assay. The Caspase-Glo 3/7 assay reagent (Promega, Madison, USA) was used for caspase detection in cells incubated with the complexes. The reagent provides a

proluminescent caspase-3/7 substrate, which contains the tethrapeptide sequence DEVD, in combination with luciferase and a cell-lysing agent. The addition of the Caspase-Glo 3/7 reagent directly to the assay well results in cell lysis, followed by caspase cleavage of the DEVD substrate, and the generation of luminescence. Caspase reagent was added directly to individual wells in white 96-well plates (1:1 ratio of Caspase reagent volume to sample volume), mixed gently on an orbital shaker for about 30 s, and further incubated at RT for 1 h prior to reading. Luminescence measurements were obtained using the FLUOstar Omega, BMG Labtech. The activity of Caspases 3/7 was calculated as arbitrary units of luminescence and expressed as percentage of control. Positive control of Caco-2 cells incubated with Staurosporine (1 μM, 4 h) was also performed to verify that the reaction was working properly.

Cell homogenates preparation. After the incubation with the complexes, the cells were resuspended and homogenized with a cold Tris-mannitol buffer (Tris 2 mM, mannitol 50 mM, pH 7.1, protease inhibitors, and 0.02% sodium azide). Then, the homogenate was disrupted by sonication (15 1-s bursts, 60 W). For lipid peroxidation and protein carbonyl analysis, the homogenate was centrifuged for 10 min at 3,000 g at 4°C and for thioredoxin reductase activity determination, the homogenate was centrifuged for 10 min at 10,000 g at 4°C. The supernatant was taken for the study. Protein content was measured by following the Bradford method (Bio-Rad, Hercules, CA, USA).

Measurement of lipid and protein oxidation. The level of lipid peroxidation was determined by measuring the concentration of malondialdehyde (MDA) and 4- hydroxyalkenals (4-HDA), as described previously.[84, 85] Briefly, MDA+4-HDA reacted with N-methyl-2-phenylindole and

yielded a stable chromophore that was measured in a spectrophotometer at 586 nm, using 1,1,3,3-tetramethoxypropane as standard. The results were calculated in nmol MDA+4-HDA mg^{-1} protein. Protein oxidation was analyzed by carbonyl level measurement as previously described.[84] Cell homogenates were incubated with the classical carbonyl reagent 2,4-dinitrophenylhydrazine (DNPH), and protein carbonylation was measured spectrophotometrically at 375 nm. The results were calculated in nmol carbonyl groups mg^{-1} protein.

Thioredoxin reductase activity. Thioredoxin reductase (TrxR) activity was determined by the Thioredoxin Reductase Assay Kit (Sigma-Aldrich, Madrid, Spain) according to the manufacturer's instructions. It is based on the reduction of 5,5′-dithiobis(2-nitrobenzoic) acid (DTNB) with NADPH to 5-thio-2-nitrobenzoic acid (TNB), which produces a strong yellow colour that is measured at 412 nm. The reaction mixture contained 50 μl of the sample, 100 mM potassium phosphate buffer at pH 7.0 with 10 mM EDTA and 0.24 mM NADPH, with and without a TrxR inhibitor, to complete a final volume of 970 μl. The reaction was started by adding 30 μl DTNB (39.6 mg mL^{-1}) and the absorbance change at 412 nm was monitored for 5 min with the spectrophotometer Hitachi U-2800A Spectrophotometer UV-vis Reader. The number of units was calculated by using Beer's Law and an extinction coefficient of 14.150 M^{-1}cm^{-1} for the TNB anion. One unit of TrxR activity is the amount of enzyme catalyzing the reduction of 1 equivalent of DTNB per min at 25 °C, pH 7 (formation of 2 equivalents of TNB anion). The specific activity of TrxR was calculated as units per mg of total protein.

Mouse model of colitis-associated cancer. All procedures were carried out under Project License PI43/17, approved by the in-house Ethics Committee for Animal Experiments from the

University of Zaragoza. The care and use of animals were performed accordingly with the Spanish Policy for Animal Protection RD53/2013, which meets the European Union Directive 2010/63 on the protection of animals used for experimental and other scientific purposes. Female Hsd:ICR (CD-1) mice (16-week-old) were purchased from Envigo (Barcelona, Spain). All mice were housed in Servicio de Experimentación Animal of the Universidad de Zaragoza, Spain, on a 12-hour light/dark cycle with food and water *ad libitum*. Mice were intraperitoneally injected with a single dose of 12 mg/kg azoxymethane (AOM) (Sigma-Aldrich, Madrid, Spain) on day 1, followed by three cycles of dextran sulfate sodium (DSS) MW 40 kDa (Sigma-Aldrich, Madrid, Spain) administration (Each cycle: 3% DSS during 5 days, followed of drinking water during 16 days), and then drinking water until the end of the experiment on weeks 10-14.

Primary cultures of mouse colonic tumors. Colonic tumors were isolated from the mice treated with the above AOM/DSS protocol (2-3 tumors/mouse) and collected in DMEM medium supplemented with 10% FBS, 100 U/mL penicillin, 100 µg/mL streptomycin, 25 µL/mL Antibiotic/Antimycotic (100x) and 50 µg/mL gentamycin. Tumors were cut into pieces and processed for enzymatic digestion in culture medium with 5 % FBS supplemented with 2 mM glutamine, insulin 4 µg/mL, dispase I 0.08 mg/mL, collagenase 0.04 mg/mL and EGF 0.01 µg/mL for 3-4 hours at 37°C in rotation. Tissue masses were washed twice, resuspended in complete medium with 25% FBS supplemented with 2 mM glutamine, insulin 4 µg/mL and EGF 0.01 µg/mL, seeded onto 96-well plates at a density of 10^5 cells per well, and incubated for 72 h at 37°C and in 5% CO_2. The medium was changed 72 h after seeding and every two days thereafter. The experiments of apoptosis (detection of phosphatidylserine with Annexin V-FITC) were carried out in the cells 7 days after seeding, following the above protocol.

Statistical Analyses. All results are expressed as means ± the standard error of the mean (SEM) of at least three independent experiments. Statistical comparisons were performed using Student's t-test or one-way ANOVA followed by the Bonferroni posttest and the differences between P-values<0.05 were considered statistically significant. Statistical analyses were carried out using the Prism GraphPad Program (Prism version 4.0, GraphPad Software, San Diego, CA).

ASSOCIATED CONTENT

Supporting Information.

Infrared spectrum of complex **1**, gold complexes stability of UV−vis absorption spectra, fluorescence emission spectra of BSA at 298 K in the presence of increasing amounts of the gold(I) complexes, and fluorescence emission spectra of the gold(I) complexes: **2**, **4-8**. Besides, crystal data and details of structure refinement for complex **4** and **5** are collected in supporting information.

AUTHOR INFORMATION

Corresponding Author

mlaguna@unizar.es (Mariano Laguna)

lgralo@unizar.es (Laura Grasa).

Author Contributions

All authors contributed equally.

Notes

REFERENCES

1.   Ferlay, J.; Soerjomataram, I.; Dikshit, R.; Eser, S.; Mathers, C.; Rebelo, M.; Parkin, D. M.; Forman, D.; Bray, F. Cancer incidence and mortality worldwide: Sources, methods and major patterns in GLOBOCAN 2012. *International Journal of Cancer* **2015,** 136 (5), E359-E386 DOI: 10.1002/ijc.29210.

2.   André, T.; Boni, C.; Mounedji-Boudiaf, L.; Navarro, M.; Tabernero, J.; Hickish, T.; Topham, C.; Zaninelli, M.; Clingan, P.; Bridgewater, J.; Tabah-Fisch, I.; de Gramont, A. Oxaliplatin, Fluorouracil, and Leucovorin as Adjuvant Treatment for Colon Cancer. *New England Journal of Medicine* **2004,** 350 (23), 2343-2351 DOI: 10.1056/NEJMoa032709.

3.   Tournigand, C.; André, T.; Bonnetain, F.; Chibaudel, B.; Lledo, G.; Hickish, T.; Tabernero, J.; Boni, C.; Bachet, J.-B.; Teixeira, L.; Gramont, A. d. Adjuvant Therapy With Fluorouracil and Oxaliplatin in Stage II and Elderly Patients (between ages 70 and 75 years) With Colon Cancer: Subgroup Analyses of the Multicenter International Study of Oxaliplatin, Fluorouracil, and Leucovorin in the Adjuvant Treatment of Colon Cancer Trial. *Journal of Clinical Oncology* **2012,** 30 (27), 3353-3360 DOI: 10.1200/jco.2012.42.5645.

4.   Mishima, M.; Samimi, G.; Kondo, A.; Lin, X.; Howell, S. B. The cellular pharmacology of oxaliplatin resistance. *European Journal of Cancer* **2002,** 38 (10), 1405-1412 DOI: 10.1016/S0959-8049(02)00096-5.

5.   Johnstone, T. C.; Suntharalingam, K.; Lippard, S. J. Third row transition metals for the treatment of cancer. *Philosophical Transactions of the Royal Society A: Mathematical, Physical and Engineering Sciences* **2015,** 373 (2037), 20140185 DOI: 10.1098/rsta.2014.0185.

6.   Miranda, S.; Vergara, E.; Mohr, F.; de Vos, D.; Cerrada, E.; Mendía, A.; Laguna, M. Synthesis, Characterization, and in Vitro Cytotoxicity of Some Gold(I) and Trans Platinum(II) Thionate Complexes Containing Water-Soluble PTA and DAPTA Ligands. X-ray Crystal Structures of [Au(SC4H3N2)(PTA)], trans-[Pt(SC4H3N2)2(PTA)2], trans-[Pt(SC5H4N)2(PTA)2], and trans-[Pt(SC5H4N)2(DAPTA)2]. *Inorganic Chemistry* **2008,** 47 (13), 5641-5648 DOI: 10.1021/ic7021903.

7.   Guerrero, E.; Miranda, S.; Lüttenberg, S.; Fröhlich, N.; Koenen, J.-M.; Mohr, F.; Cerrada, E.; Laguna, M.; Mendía, A. trans-Thionate Derivatives of Pt(II) and Pd(II) with Water-Soluble Phosphane PTA and DAPTA Ligands: Antiproliferative Activity against Human Ovarian Cancer Cell Lines. *Inorganic Chemistry* **2013,** 52 (11), 6635-6647 DOI: 10.1021/ic4006746.

8.   Shaw, C. F. Gold-Based Therapeutic Agents. *Chemical Reviews* **1999,** 99 (9), 2589-2600 DOI: 10.1021/cr980431o.

9.   Simon, T. M.; Kunishima, D. H.; Vibert, G. J.; Lorber, A. Screening Trial with the Coordinated Gold Compound Auranofin Using Mouse Lymphocytic Leukemia P388. *Cancer Research* **1981,** 41 (1), 94.

10.   Mirabelli, C. K.; Johnson, R. K.; Sung, C. M.; Faucette, L.; Muirhead, K.; Crooke, S. T. Evaluation of the in vivo antitumor activity and in vitro cytotoxic properties of auranofin, a coordinated gold compound, in murine tumor models. *Cancer Res* **1985,** 45 (1), 32-9.

11.   Bagowski, C. P.; You, Y.; Scheffler, H.; Vlecken, D. H.; Schmitz, D. J.; Ott, I. Naphthalimide gold(i) phosphine complexes as anticancer metallodrugs. *Dalton Transactions* **2009,** (48), 10799-10805 DOI: 10.1039/B912378D.

12.   Ott, I.; Qian, X.; Xu, Y.; Vlecken, D. H. W.; Marques, I. J.; Kubutat, D.; Will, J.; Sheldrick, W. S.; Jesse, P.; Prokop, A.; Bagowski, C. P. A Gold(I) Phosphine Complex Containing a Naphthalimide Ligand Functions as a TrxR Inhibiting Antiproliferative Agent and Angiogenesis Inhibitor. *Journal of Medicinal Chemistry* **2009,** 52 (3), 763-770 DOI: 10.1021/jm8012135.

13.   Ortego, L.; Cardoso, F.; Martins, S.; Fillat, M. F.; Laguna, A.; Meireles, M.; Villacampa, M. D.; Gimeno, M. C. Strong inhibition of thioredoxin reductase by highly cytotoxic gold(I) complexes. DNA binding studies. *Journal of Inorganic Biochemistry* **2014,** 130, 32-37 DOI: 10.1016/j.jinorgbio.2013.09.019.

14.   Atrián-Blasco, E.; Gascón, S.; Rodríguez-Yoldi, M. J.; Laguna, M.; Cerrada, E. Novel Gold(I) Thiolate Derivatives Synergistic with 5-Fluorouracil as Potential Selective Anticancer Agents in Colon Cancer. *Inorganic Chemistry* **2017,** 56 (14), 8562-8579 DOI: 10.1021/acs.inorgchem.7b01370.

15.   García-Moreno, E.; Tomás, A.; Atrián-Blasco, E.; Gascón, S.; Romanos, E.; Rodriguez-Yoldi, M. J.; Cerrada, E.; Laguna, M. In vitro and in vivo evaluation of organometallic gold(i) derivatives as anticancer agents. *Dalton Transactions* **2016,** 45 (6), 2462-2475 DOI: 10.1039/C5DT01802A.

16.   Elena, G.-M.; Sonia, G.; Jose, A. G. d. J.; Eduardo, R.; Rodriguez-Yoldi, M. J.; Elena, C.; Mariano, L. In Vivo Anticancer Activity, Toxicology and Histopathological Studies of the Thiolate Gold(I) Complex [Au(Spyrimidine)(PTA-CH$_2$Ph)]Br. *Anti-Cancer Agents in Medicinal Chemistry* **2015,** 15 (6), 773-782 DOI: 10.2174/1871520615666150129211440.

17.   García-Moreno, E.; Gascón, S.; Atrián-Blasco, E.; Rodriguez-Yoldi, M. J.; Cerrada, E.; Laguna, M. Gold(I) complexes with alkylated PTA (1,3,5-triaza-7-phosphaadamantane) phosphanes as anticancer metallodrugs. *European Journal of Medicinal Chemistry* **2014,** 79, 164-172 DOI: 10.1016/j.ejmech.2014.04.001.

18.   Vergara, E.; Casini, A.; Sorrentino, F.; Zava, O.; Cerrada, E.; Rigobello, M. P.; Bindoli, A.; Laguna, M.; Dyson, P. J. Anticancer therapeutics that target selenoenzymes: synthesis, characterization, in vitro cytotoxicity, and thioredoxin reductase inhibition of a series of gold(I) complexes containing hydrophilic phosphine ligands. *ChemMedChem* **2010,** 5 (1), 96-102 DOI: 10.1002/cmdc.200900370.

19.   Vergara, E.; Cerrada, E.; Clavel, C.; Casini, A.; Laguna, M. Thiolato gold(I) complexes containing water-soluble phosphane ligands: a characterization of their chemical and biological

properties. *Dalton transactions (Cambridge, England : 2003)* **2011,** 40 (41), 10927-35 DOI: 10.1039/c1dt10892a.

20.   Bertrand, B.; Spreckelmeyer, S.; Bodio, E.; Cocco, F.; Picquet, M.; Richard, P.; Le Gendre, P.; Orvig, C.; Cinellu, M. A.; Casini, A. Exploring the potential of gold(iii) cyclometallated compounds as cytotoxic agents: variations on the C^N theme. *Dalton Transactions* **2015,** 44 (26), 11911-11918 DOI: 10.1039/C5DT01023C.

21.   Vergara, E.; Cerrada, E.; Casini, A.; Zava, O.; Laguna, M.; Dyson, P. J. Antiproliferative Activity of Gold(I) Alkyne Complexes Containing Water-Soluble Phosphane Ligands. *Organometallics* **2010,** 29 (11), 7.

22.   Meyer, A.; Bagowski, C. P.; Kokoschka, M.; Stefanopoulou, M.; Alborzinia, H.; Can, S.; Vlecken, D. H.; Sheldrick, W. S.; Wölfl, S.; Ott, I. On the Biological Properties of Alkynyl Phosphine Gold(I) Complexes. *Angewandte Chemie International Edition* **2012,** 51 (35), 8895-8899 DOI: 10.1002/anie.201202939.

23.   Schuh, E.; Valiahdi, S. M.; Jakupec, M. A.; Keppler, B. K.; Chiba, P.; Mohr, F. Synthesis and biological studies of some gold(I) complexes containing functionalised alkynes. *Dalton Transactions* **2009,** (48), 10841-10845 DOI: 10.1039/B911234K.

24.   Ganga Reddy, V.; Srinivasa Reddy, T.; Privér, S. H.; Bai, Y.; Mishra, S.; Wlodkowic, D.; Mirzadeh, N.; Bhargava, S. Synthesis of Gold(I) Complexes Containing Cinnamide: In Vitro Evaluation of Anticancer Activity in 2D and 3D Spheroidal Models of Melanoma and In Vivo Angiogenesis. *Inorganic Chemistry* **2019,** 58 (9), 5988-5999 DOI: 10.1021/acs.inorgchem.9b00281.

25.   Balasingham, R. G.; Williams, C. F.; Mottram, H. J.; Coogan, M. P.; Pope, S. J. A. Gold(I) Complexes Derived from Alkynyloxy-Substituted Anthraquinones: Syntheses, Luminescence, Preliminary Cytotoxicity, and Cell Imaging Studies. *Organometallics* **2012,** 31 (16), 5835-5843 DOI: 10.1021/om300475y.

26.   Meyer, A.; Bagowski, C. P.; Kokoschka, M.; Stefanopoulou, M.; Alborzinia, H.; Can, S.; Vlecken, D. H.; Sheldrick, W. S.; Wölfl, S.; Ott, I. Über die biologischen Eigenschaften von Alkinyl(phosphan)gold(I)-Komplexen. *Angewandte Chemie* **2012,** 124 (35), 9025-9030 DOI: 10.1002/ange.201202939.

27.   Bertrand, B.; Casini, A. A golden future in medicinal inorganic chemistry: the promise of anticancer gold organometallic compounds. *Dalton Transactions* **2014,** 43 (11), 4209-4219 DOI: 10.1039/C3DT52524D.

28.   Mármol, I.; Castellnou, P.; Alvarez, R.; Gimeno, M. C.; Rodríguez-Yoldi, M. J.; Cerrada, E. Alkynyl Gold(I) complexes derived from 3-hydroxyflavones as multi-targeted drugs against colon cancer. *European Journal of Medicinal Chemistry* **2019,** 183, 111661 DOI: 10.1016/j.ejmech.2019.111661.

29.   Yeo, C. I.; Ooi, K. K.; Tiekink, E. R. T. Gold-Based Medicine: A Paradigm Shift in Anti-Cancer Therapy? *Molecules* **2018,** 23 (6), DOI: 10.3390/molecules23061410.

30.   Fan, C.; Zheng, W.; Fu, X.; Li, X.; Wong, Y. S.; Chen, T. Enhancement of auranofin-induced lung cancer cell apoptosis by selenocystine, a natural inhibitor of TrxR1 in vitro and in vivo. *Cell death & disease* **2014,** 5 (4), e1191-e1191 DOI: 10.1038/cddis.2014.132.

31.   Koharyova, M.; Kollarova, M. Thioredoxin system - a novel therapeutic target. *General physiology and biophysics* **2015,** 34 (3), 221-33 DOI: 10.4149/gpb_2015006.

32.   Karlenius, T. C.; Tonissen, K. F. Thioredoxin and Cancer: A Role for Thioredoxin in all States of Tumor Oxygenation. *Cancers* **2010,** 2 (2), 209-232.

33. Polimeni, M.; Gazzano, E. Is redox signaling a feasible target for overcoming multidrug resistance in cancer chemotherapy? *Frontiers in Pharmacology* **2014,** 5 (286), DOI: 10.3389/fphar.2014.00286.

34. Bauer, A.; Mitzel, N. W.; Schier, A.; Schmidbaur, H.; Rankin, D. W. H. Tris(dimethylamino)phosphane as a New Ligand in Gold(I) Chemistry: Synthesis and Crystal Structures of $[(Me_2N)_3P]AuCl$, $\{[(Me_2N)_3PAu]_3O\}^+BF_4^-$, $\{[(Me_2N)_3PAu]_3NP(NMe_2)_3^{2+} \{BF^-\}_2$ and the Precursor Molecule $(Me_2N)_3PNSiMe_3$. *Chemische Berichte* **1997,** 30 (4), 5.

35. Schuster, O.; Liau, R.-Y.; Schier, A.; Schmidbaur, H. Preparation, structure and decomposition of gold(I) and gold(III) acetylide complexes. *Inorganica Chimica Acta* **2005,** 358 (5), 1429-1441 DOI: 10.1016/j.ica.2004.07.005.

36. Boscutti, G.; Nardon, C.; Marchio, L.; Crisma, M.; Biondi, B.; Dalzoppo, D.; Dalla Via, L.; Formaggio, F.; Casini, A.; Fregona, D. Anticancer Gold(III) Peptidomimetics: From Synthesis to in vitro and ex vivo Biological Evaluations. *ChemMedChem* **2018,** 13 (11), 1131-1145 DOI: 10.1002/cmdc.201800098.

37. Cheng, A.; Merz, K. M. Prediction of Aqueous Solubility of a Diverse Set of Compounds Using Quantitative Structure−Property Relationships. *Journal of Medicinal Chemistry* **2003,** 46 (17), 3572-3580 DOI: 10.1021/jm020266b.

38. Lombardo, F.; Obach, R. S.; Shalaeva, M. Y.; Gao, F. Prediction of Volume of Distribution Values in Humans for Neutral and Basic Drugs Using Physicochemical Measurements and Plasma Protein Binding Data. *Journal of Medicinal Chemistry* **2002,** 45 (13), 2867-2876 DOI: 10.1021/jm0200409.

39. Kerns, E. H.; Di, L. In *Lipophilicity Methods*; Elsevier: San Diego, 2008; Chapter 23, p 10.

40. Huang, H.; Zhang, P.; Yu, B.; Chen, Y.; Wang, J.; Ji, L.; Chao, H. Targeting Nucleus DNA with a Cyclometalated Dipyridophenazineruthenium(II) Complex. *Journal of Medicinal Chemistry* **2014,** 57 (21), 8971-8983 DOI: 10.1021/jm501095r.

41. McKeage, M. J.; Berners-Price, S. J.; Galettis, P.; Bowen, R. J.; Brouwer, W.; Ding, L.; Zhuang, L.; Baguley, B. C. Role of lipophilicity in determining cellular uptake and antitumour activity of gold phosphine complexes. *Cancer Chemotherapy and Pharmacology* **2000,** 46 (5), 343-350 DOI: 10.1007/s002800000166.

42. Berners-Price, S. J.; Filipovska, A. The Design of Gold-Based, Mitochondria-Targeted Chemotherapeutics. *Australian Journal of Chemistry* **2008,** 61 (9), 661-668 DOI: 10.1071/CH08175.

43. Bhal, S. K. LogP: Making Sense of the Value. http://www.acdlabs.com/resources/knowledgebase/app_notes/-physchem/makingsense.php (June 17, 2018),

44. Tasaioun, K.; Kates, S. A. *ADMET for Medicinal Chemists: A partical guide*. John Wiley & Sons, Inc. Hoboken, New Jersey, 2010; Vol. 1.

45. Anand, U.; Mukherjee, S. Binding, unfolding and refolding dynamics of serum albumins. *Biochim Biophys Acta* **2013,** 1830 (12), 5394-404 DOI: 10.1016/j.bbagen.2013.05.017.

46. Yamasaki, K.; Chuang, V. T.; Maruyama, T.; Otagiri, M. Albumin-drug interaction and its clinical implication. *Biochim Biophys Acta* **2013,** 1830 (12), 5435-43 DOI: 10.1016/j.bbagen.2013.05.005.

47. Smith, D. A.; Van de waterbeemd, H.; Walker, D. K. *Pharmacokinetics and Metabolism in Drug Design*. Wiley-VCH Verlag & Co. Weinheim, 2012.

48.   Anguizola, J.; Matsuda, R.; Barnaby, O. S.; Hoy, K. S.; Wa, C.; DeBolt, E.; Koke, M.; Hage, D. S. Review: Glycation of human serum albumin. *Clin Chim Acta* **2013,** 425, 64-76 DOI: 10.1016/j.cca.2013.07.013.

49.   Lakowicz, J. R. In *Principles of Fluorescence Spectroscopy*; 3rd ed.; Springer, New York. 2006; Chapter 8, Vol. 1, pp 277-310.

50.   Neault, J. F.; Tajmir-Riahi, H. A. Interaction of cisplatin with human serum albumin. Drug binding mode and protein secondary structure. *Bba-Protein Struct M* **1998,** 1384 (1), 153-159 DOI: Doi 10.1016/S0167-4838(98)00011-9.

51.   Suryawanshi, V. D.; Walekar, L. S.; Gore, A. H.; Anbhule, P. V.; Kolekar, G. B. Spectroscopic analysis on the binding interaction of biologically active pyrimidine derivative with bovine serum albumin. *J Pharm Ana* **2016,** 6 (1), 56-63 DOI: 10.1016/j.jpha.2015.07.001.

52.   Meunier, V.; Bourrié, M.; Berger, Y.; Fabre, G. The human intestinal epithelial cell line Caco-2; pharmacological and pharmacokinetic applications. *Cell Biology and Toxicology* **1995,** 11 (3), 187-194 DOI: 10.1007/bf00756522.

53.   Mesonero, J.; Mahraoui, L.; Matosin, M.; Rodolosse, A.; Rousset, M.; Brot-Laroche, E. *Expression or the hexose transporters GLUT1–GLUT5 and SGLT1 in clones of Caco–2 cells.* 1994; Vol. 22, p 681-4.

54.   Rousset, M. The human colon carcinoma cell lines HT-29 and Caco-2: Two in vitro models for the study of intestinal differentiation. *Biochimie* **1986,** 68 (9), 1035-1040 DOI: 10.1016/S0300-9084(86)80177-8.

55.   Mosmann, T. Rapid colorimetric assay for cellular growth and survival: application to proliferation and cytotoxicity assays. *J Immunol Methods* **1983,** 65 (1-2), 55-63.

56.   Vaux, D. L.; Korsmeyer, S. J. Cell death in development. *Cell* **1999,** 96 (2), 245-54.

57.   Bennett, M. R.; Gibson, D. F.; Schwartz, S. M.; Tait, J. F. Binding and phagocytosis of apoptotic vascular smooth muscle cells is mediated in part by exposure of phosphatidylserine. *Circ Res* **1995,** 77 (6), 1136-42.

58.   Fadok, V. A.; Bratton, D. L.; Frasch, S. C.; Warner, M. L.; Henson, P. M. The role of phosphatidylserine in recognition of apoptotic cells by phagocytes. *Cell Death Differ* **1998,** 5 (7), 551-62 DOI: 10.1038/sj.cdd.4400404.

59.   Fadok, V. A.; Voelker, D. R.; Campbell, P. A.; Cohen, J. J.; Bratton, D. L.; Henson, P. M. Exposure of phosphatidylserine on the surface of apoptotic lymphocytes triggers specific recognition and removal by macrophages. *J Immunol* **1992,** 148 (7), 2207-16.

60.   Mower, D. A., Jr.; Peckham, D. W.; Illera, V. A.; Fishbaugh, J. K.; Stunz, L. L.; Ashman, R. F. Decreased membrane phospholipid packing and decreased cell size precede DNA cleavage in mature mouse B cell apoptosis. *J Immunol* **1994,** 152 (10), 4832-42.

61.   Elmore, S. Apoptosis: a review of programmed cell death. *Toxicol Pathol* **2007,** 35 (4), 495-516 DOI: 10.1080/01926230701320337.

62.   Igney, F. H.; Krammer, P. H. Death and anti-death: tumour resistance to apoptosis. *Nat Rev Cancer* **2002,** 2 (4), 277-88 DOI: 10.1038/nrc776.

63.   Kuranaga, E. Beyond apoptosis: caspase regulatory mechanisms and functions in vivo. *Genes Cells* **2012,** 17 (2), 83-97 DOI: 10.1111/j.1365-2443.2011.01579.x.

64.   Taylor, R. C.; Cullen, S. P.; Martin, S. J. Apoptosis: controlled demolition at the cellular level. *Nature Reviews Molecular Cell Biology* **2008,** 9, 231 DOI: 10.1038/nrm2312

65.   Cronje, S.; Raubenheimer, H. G.; Spies, H. S. C.; Esterhuysen, C.; Schmidbaur, H.; Schier, A.; Kruger, G. J. Synthesis and characterisation of N-coordinated pentafluorophenyl gold(i)

thiazole-derived complexes and an unusual self-assembly to form a tetrameric gold(i) complex. *Dalton Transactions* **2003,** (14), 2859-2866 DOI: 10.1039/B303625A.

66.　　de Jongh, L.-A.; Dobrzańska, L.; Strasser Christoph, E.; Raubenheimer Helgard, G.; Cronje, S., Imine-coordinated 2-Aminoazole Complexes of Au(I): Complicating Reactions and Verification of Products by Crystal Structure Determination. In *Zeitschrift für Naturforschung B*, 2014; Vol. 69, p 1073.

67.　　Li, X.; Wang, G.; Zhao, J.; Ding, H.; Cunningham, C.; Chen, F.; Flynn, D. C.; Reed, E.; Li, Q. Q. Antiproliferative effect of β-elemene in chemoresistant ovarian carcinoma cells is mediated through arrest of the cell cycle at the G2-M phase. *Cellular and Molecular Life Sciences CMLS* **2005,** 62 (7), 894-904 DOI: 10.1007/s00018-005-5027-1.

68.　　Schieber, M.; Chandel, Navdeep S. ROS Function in Redox Signaling and Oxidative Stress. *Current Biology* **2014,** 24 (10), R453-R462 DOI: 10.1016/j.cub.2014.03.034.

69.　　Halliwell, B.; Chirico, S. Lipid peroxidation: its mechanism, measurement, and significance. *The American Journal of Clinical Nutrition* **1993,** 57 (5), 715S-725S DOI: 10.1093/ajcn/57.5.715S.

70.　　Levine, R. L. Carbonyl modified proteins in cellular regulation, aging, and disease. *Free Radical Biology and Medicine* **2002,** 32 (9), 790-796 DOI: 10.1016/S0891-5849(02)00765-7.

71.　　Matsui, A.; Ikeda, T.; Enomoto, K.; Hosoda, K.; Nakashima, H.; Omae, K.; Watanabe, M.; Hibi, T.; Kitajima, M. Increased formation of oxidative DNA damage, 8-hydroxy-2′-deoxyguanosine, in human breast cancer tissue and its relationship to GSTP1 and COMT genotypes. *Cancer Letters* **2000,** 151 (1), 87-95 DOI: 10.1016/S0304-3835(99)00424-3.

72.　　Shacter, E. Protein oxidative damage In *Methods in Enzymology*; Academic Press, Elsevier: La Jolla, CA, USA 2000; Vol. 319, pp 428-436.

73.　　Gérard-Monnier, D.; Erdelmeier, I.; Régnard, K.; Moze-Henry, N.; Yadan, J.-C.; Chaudière, J. Reactions of 1-Methyl-2-phenylindole with Malondialdehyde and 4-Hydroxyalkenals. Analytical Applications to a Colorimetric Assay of Lipid Peroxidation. *Chemical Research in Toxicology* **1998,** 11 (10), 1176-1183 DOI: 10.1021/tx9701790.

74.　　He, L.; He, T.; Farrar, S.; Ji, L.; Liu, T.; Ma, X. Antioxidants Maintain Cellular Redox Homeostasis by Elimination of Reactive Oxygen Species. *Cell Physiol Biochem* **2017,** 44 (2), 532-553 DOI: 10.1159/000485089.

75.　　Zhang, J.; Li, X.; Han, X.; Liu, R.; Fang, J. Targeting the Thioredoxin System for Cancer Therapy. *Trends Pharmacol Sci* **2017,** 38 (9), 794-808 DOI: 10.1016/j.tips.2017.06.001.

76.　　Bertrand, B.; Citta, A.; Franken, I. L.; Picquet, M.; Folda, A.; Scalcon, V.; Rigobello, M. P.; Le Gendre, P.; Casini, A.; Bodio, E. Gold(I) NHC-based homo- and heterobimetallic complexes: synthesis, characterization and evaluation as potential anticancer agents. *JBIC Journal of Biological Inorganic Chemistry* **2015,** 20 (6), 1005-1020 DOI: 10.1007/s00775-015-1283-1.

77.　　Luthman, M.; Holmgren, A. Rat liver thioredoxin and thioredoxin reductase: purification and characterization. *Biochemistry* **1982,** 21 (26), 6628-6633 DOI: 10.1021/bi00269a003.

78.　　De Robertis, M.; Massi, E.; Poeta, M. L.; Carotti, S.; Morini, S.; Cecchetelli, L.; Signori, E.; Fazio, V. M. The AOM/DSS murine model for the study of colon carcinogenesis: From pathways to diagnosis and therapy studies. *Journal of carcinogenesis* **2011,** 10, 9-9 DOI: 10.4103/1477-3163.78279.

79.　　Parang, B.; Barrett, C. W.; Williams, C. S. AOM/DSS Model of Colitis-Associated Cancer. In *Gastrointestinal Physiology and Diseases: Methods and Protocols*; Ivanov, A. I., Ed.; Springer New York: New York, NY, 2016; pp 297-307.

80. Uson, R.; Laguna, A.; Laguna, M.; Briggs, D. A.; Murray, H. H.; Fackler, J. P. (Tetrahydrothiophene)Gold(I) or Gold(III) Complexes. *Inorg. Synth.* **2007,** 26, 7 DOI: 10.1002/9780470132579.ch17.

81. Farrugia, L. WinGX suite for small-molecule single-crystal crystallography. *Journal of Applied Crystallography* **1999,** 32 (4), 837-838 DOI: 10.1107/S0021889899006020.

82. Mesonero, J.; Mahraoui, L.; Matosin, M.; Rodolosse, A.; Rousset, M.; Brot-Laroche, E. Expression of the hexose transporters GLUT1-GLUT5 and SGLT1 in clones of Caco-2 cells. *Biochemical Society transactions* **1994,** 22 (3), 681-4.

83. Zucco, F.; Batto, A. F.; Bises, G.; Chambaz, J.; Chiusolo, A.; Consalvo, R.; Cross, H.; Dal Negro, G.; de Angelis, I.; Fabre, G.; Guillou, F.; Hoffman, S.; Laplanche, L.; Morel, E.; Pincon-Raymond, M.; Prieto, P.; Turco, L.; Ranaldi, G.; Rousset, M.; Sambuy, Y.; Scarino, M. L.; Torreilles, F.; Stammati, A. An inter-laboratory study to evaluate the effects of medium composition on the differentiation and barrier function of Caco-2 cell lines. *Altern Lab Anim* **2005,** 33 (6), 603-18.

84. Gonzalo, S.; Grasa, L.; Arruebo, M. P.; Plaza, M. A.; Murillo, M. D. Extracellular signal-regulated kinase (ERK) is involved in LPS-induced disturbances in intestinal motility. *Neurogastroenterol Motil* **2011,** 23 (2), 80-90 DOI: 10.1111/j.1365-2982.2010.01632.x.

85. Latorre, E.; Mendoza, C.; Layunta, E.; Alcalde, A. I.; Mesonero, J. E. TLR2, TLR3, and TLR4 activation specifically alters the oxidative status of intestinal epithelial cells. *Cell Stress Chaperones* **2014,** 19 (2), 289-93 DOI: 10.1007/s12192-013-0461-8.

Efficiency and selectivity

Mechanism of action
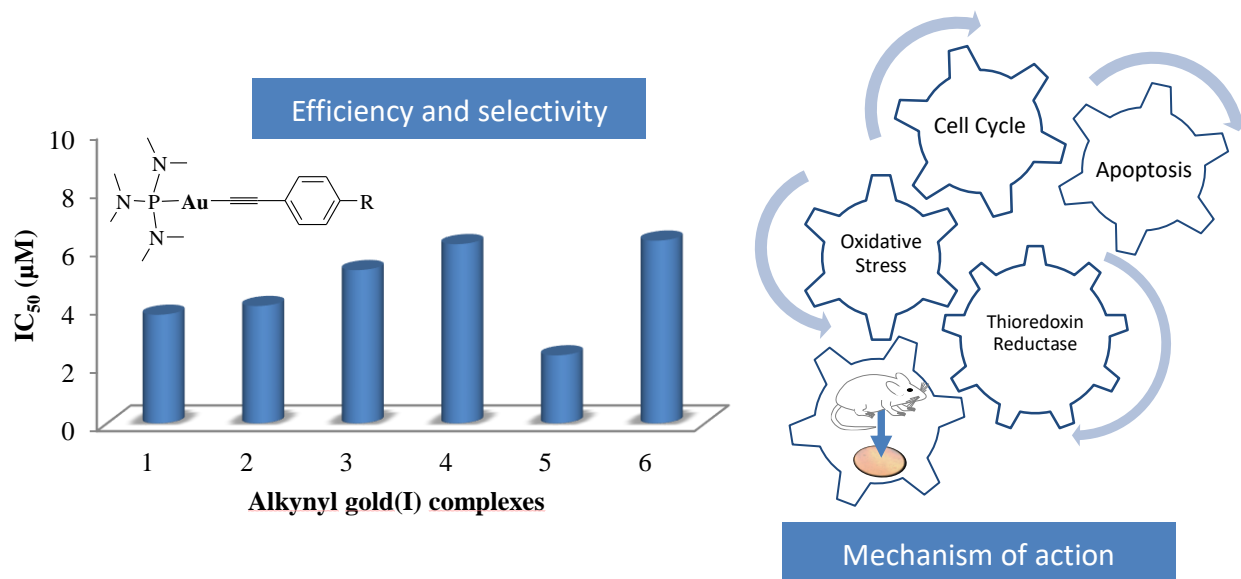
A total of five gold(I) complexes are selective to tumor cells (Caco-2) by apoptosis processes. This cell death seems to be promoted by inhibition of TrxR system which induces an oxidative stress damage in membrane lipids.